REPORT DOCUMENTATION PAGE

Form Approved OMB NO. 0704-0188

1. REPORT DATE (DD-MM-YYYY)	2. REPORT TYPE	3. DATES COVERED (From - To)
18-12-2019	Final Report	1-Sep-2015 - 31-Aug-2019

4. TITLE AND SUBTITLE
Final Report: Optical and Electrical Properties of NiFe-oxide Thin Films

5a. CONTRACT NUMBER
W911NF-15-1-0394

5b. GRANT NUMBER

5c. PROGRAM ELEMENT NUMBER
106012

6. AUTHORS

5d. PROJECT NUMBER

5e. TASK NUMBER

5f. WORK UNIT NUMBER

7. PERFORMING ORGANIZATION NAMES AND ADDRESSES

Texas State University
601 University Drive, JCK 420

San Marcos, TX 78666 -4864

8. PERFORMING ORGANIZATION REPORT NUMBER

9. SPONSORING/MONITORING AGENCY NAME(S) AND ADDRESS (ES)

U.S. Army Research Office
P.O. Box 12211
Research Triangle Park, NC 27709-2211

10. SPONSOR/MONITOR'S ACRONYM(S)
ARO

11. SPONSOR/MONITOR'S REPORT NUMBER(S)
67340-MS-REP.45

12. DISTRIBUTION AVAILIBILITY STATEMENT

Approved for public release; distribution is unlimited.

13. SUPPLEMENTARY NOTES

The views, opinions and/or findings contained in this report are those of the author(s) and should not contrued as an official Department of the Army position, policy or decision, unless so designated by other documentation.

14. ABSTRACT

15. SUBJECT TERMS

16. SECURITY CLASSIFICATION OF:			17. LIMITATION OF ABSTRACT	15. NUMBER OF PAGES	19a. NAME OF RESPONSIBLE PERSON
a. REPORT	b. ABSTRACT	c. THIS PAGE			Wim Geerts
UU	UU	UU	UU		19b. TELEPHONE NUMBER 512-245-1821

RPPR Final Report
as of 03-Jan-2020

Agency Code:

Proposal Number: 67340MSREP **Agreement Number: W911NF-15-1-0394**
INVESTIGATOR(S):

Name: Luisa Scolfaro
Email: ls61@txstate.edu
Phone Number: 5122452102
Principal: N

Name: Wim Geerts
Email: wg06@txstate.edu
Phone Number: 5122451821
Principal: Y

Organization: **Texas State University**
Address: 601 University Drive, JCK 420, San Marcos, TX 786664864
Country: USA
DUNS Number: 074602368 EIN: 746002248

Report Date: 30-Nov-2019 Date Received: 18-Dec-2019
Final Report for Period Beginning 01-Sep-2015 and Ending 31-Aug-2019
Title: Optical and Electrical Properties of NiFe-oxide Thin Films
Begin Performance Period: 01-Sep-2015 **End Performance Period:** 31-Aug-2019
Report Term: 0-Other

Submitted By: Wim Geerts Email: wg06@txstate.edu
Phone: (512) 245-1821

STEM Degrees: 10 **STEM Participants:** 14

Major Goals: The objective of this research project was to conduct fundamental research to better understand electronic transport in RF sputtered Fe doped nickel oxide thin films for application in radiation-hard, low-energy, high-speed logic resistive-memory devices. A complementary experimental and theoretical approach was followed to investigate the optical and electrical transport properties of RF sputtered NiFe-oxide thin films and their applicability to RRAM devices.
Experimental goals:
(1) structural and chemical characterization using XRD, EDAX, XPS and RBS.
(2) optical characterization using FTIR, ellipsometry, and optical transmission measurements.
(3) electrical characterization including four and two-point probe IV measurements, CV measurements, and DLTS measurements. Samples are continuous thin films and devices. Experiments are supplemented by device computations using the finite element technique.
(4) magnetic characterization using VSM, Magneto-Optical Kerr magnetometry, and MFM.
Theoretical goals:
DFT calculations to better understand the electronic structure and ion mobility of NiO and doped NiO. In particularly the effect of iron-doping and vacancies on the optical, magnetic, and electrical properties.

Accomplishments: see attached final report in the upload section

Training Opportunities: Ahad Talukder (MSEC PhD student, Geerts, 9/18-1/19): Ahad, a 2nd year MSEC PhD student did a collaborative research class with me in the Fall 2018 semester. He did IVT measurements and dlts measurements on oxygen low samples. The IVT show freeze out at low temperature and the dlts did not show any peaks. IVT measurements on films and dlts measurements on high oxygen films are scheduled.

James Nick Talbert (MSc, Geerts, 9/18-11/19): Nick worked with the PI on electrical characterization of NiFeO-heterojunctions and charge transport in NiFeO thin films. His thesis project has been the most challenging project in the PI's lab as initially the data of the device wafers were very scattered. Only after modifications were made to the deposition process, he was able to see a pattern. He finished and defended thesis in Nov. 2019. Part of his work was presented the Fall-2018 TSAP meeting in Houston and the MRS conference in Phoenix and published in an MRS conference paper. Nick is currently working on his resume and applying for jobs in industry in the Austin-San Antonio corridor.

Sam Cantrell (MSc, Scolfaro, 9/18-11/19): Sam worked with the Co-Pi on Density Functional Theory calculations using the VASP code of doped NiO system and included doping with Cu, Ag, and C. For the C doped case he investigated the effect of C on an Oxygen site and C on a Ni site. In addition, he investigated the effect of Ni vacancies in NiFeO, oxygen and Ni interstitial in NiO, neutral oxygen vacancies in NiO and positively charged oxygen vacancies in NiO. Part of his work was presented at the TSAPS-2018 Fall meeting in Houston, the April APS-2019 meeting in Houston and the Wise-2019 meeting at Texas State University. He finished his thesis and defended in Nov. 2019. In addition to his thesis work, he supported the MRS paper of grad. student Nick Talbert with calculations that show that oxygen vacancies in NiO are localized which earned him a co-authorship. Sam co-coached Lauren Trombley, the 2019 URAP intern working in Dr. Scolfaro's lab. He is currently employed at the University doing DFT calculations for Dr. Zakhidov while applying for PhD programs for Fall 2019.

Binod D.C. (MSc, Geerts, 9/18-8/19): Binod worked with the PI on XPS, Xray, and magnetic characterization of NiFeO thin films. In addition he verified the new Vibrating Sample Magnetometer tool that we won on an NSF-MRI grant. He submitted and defended his thesis in Aug. 2019. Part of his thesis work was presented at the TSAPS Spring-2018 meeting, the TSAPS Spring-2019 meeting, and the International Conference on Magnetism in San Francisco in July 2018. Part of his thesis is published in IEEE Trans. on Magn. in Fall 2018. Part of his thesis work involving the verification of the VSM led to a new method to determine the sample position in a VSM. This invention is currently being disclosed to the University. Binod co-coached Sarah-Beth Ragan, the 2019 HSAP intern with the PI. In the Fall 2019 semester he joined the group of Dr. Yoichi Miyahara as an MSEC-Phd student from Fall 2019.

Shankar Acharya (MSc, Geerts, 9/18-8/19): Worked with the PI on the Magneto-Optical characterization of NiFeO thin films. Together with undergraduate student Brian Collier, he built a dual beam MOKE setup that was used to measure the Faraday hysteresis curves of NiFeO thin films. He submitted and defended his thesis in May 2019. Part of his thesis was presented at 4 different conferences and published in Review of Scientific Instruments in December 2019. He is currently employed with NXP Semiconductor in Austin Texas.

Rigoberto Mayorga-Luna (undergrad, Geerts, 09/18-05/19): Has done an independent study with the PI in the Fall 2018 semester and extended the linear four-point probe Labview program to include a routine to double check the contacts from 2pp measurements. His program allows to identify up to two troubled contacts. He presented this work at the Wise conference in Spring 2019. He graduated in May 2019 and taught labs for us during the fall-2019 semester. He applied to graduate school and will enroll in January if his financial situation permits it. He is currently also applying for DOD internship for the summer of 2020.

Clint Boldt (undergrad, Geerts, 9/18-9/19): Clint worked in the fall-2018 with graduate student Ahad Talukder on the DLTS/IVT setup. He attended the TSAPS Fall-2018 meeting to present a poster on hid work and took graduate EMT with me in the spring 2019 semester for honor's undergraduate credit. He did well in that class. He graduated in May 2019 and is currently applying to graduate school including, UTSA, Rice, University of Colorado at Boulder, and University of Denver. He is very interested in BioPhysics.

Salamon Gallegos (undergrad, Geerts 6/18-12/18): refurbished the laserbeamwriter setup for an independent research class. Activities included: fixed hinges on doors on the unit, transferred the stepmotor card and software to a 64 bits windows computer and found the correct drivers, re-connected the power lines, reconnected the light sources of the background light and the alignment beam, determined the problem with the camera and installed the fixed camera on the new computer. He graduated in Dec. 2018 and is currently working for SRC, a defense contractor

RPPR Final Report
as of 03-Jan-2020

Noel Gamez (undergrad, Geerts, 9/18-5/19): Noel took two more class in the Fall 2018 and spring 2019 semesters, studied for the GRE exam, and applied to graduate programs. Last class he took in the spring was graduate Electromagnetic Field Theory. He graduated in May 2019. He started on his PhD at Baylor University in Fall 2019. In the Fall-2018 semester he presented his research work at the TSAPS-Fall meeting in Houston and at the UT Symposium for Undergraduate Research Exploration 2018.

Sarah-Beth Ragan (high school, Geerts, 6/19-9/19): Sarah-Beth was a HSAP intern in the summer of 2019. She worked on the magnetic characterization of NiFeO, 3D printed magnetic PLA, and various magnetic tapes and floppy samples. Project focus was on angular measurements and how sample shape and alignment affect the angular dependence of the magnetic properties. She worked closely together with graduate student Binod D.C.. Part of her results were presented at the TSAPS Fall-2019 meeting in Lubbock.

Lauren Trombley (undergrad, Scolfaro, 6/19-9/19): Lauren was a URAP intern in the summer of 2019 and worked with Dr. Scolfaro and graduate student Sam Cantrell on DFT calculations on the thermodynamic properties of pristine NiO. Lauren used the VASP package and Gibbs2 computational program. Her project was finished with a 13-page technical report. Lauren graduated in May 2019.

Sam Zamora: (undergrad, Geerts 9/18-11/19): Continued his work on the magnetic properties of 3D printed magnetic PLA. He presented a poster at the TSAPS spring 2019 meeting and is currently writing a paper on his work. Sam is a stellar student and intends to enlist with the Navy upon graduation. He finished his Navy fitness test in early November.

Selena Rose Najar (undergrad, Geerts, 8/18-8/19): Rose is working on the magnetic properties of annealed NiFeO films. She discovered that annealing the sample in a field at 600 or 700 C results in a phase transformation of part of the film. She is currently exploring the magnetic anisotropy developed by these field anneals. She presented her research at the TSAPS Fall-2018 meeting, the Symposium for Undergraduate Research Exploration 2018 at UT, and the Wise 2019 conference at Texas State. Rose expects to graduate in May 2020. She is currently applying to graduate programs.

Kolton Dieckow (MSc, Geerts 8/19-): Kolton is working on angular torque measurements done with the biaxial VSM to determine the effect of field anneals on NiFeO thin films. He presented a poster at the FALL-2019 TSAPS meeting of his results and the results of Binod and Sarah-Beth obtained in the summer of 2019. He expects to graduate in December 2020.

RPPR Final Report
as of 03-Jan-2020

Results Dissemination: The work has resulted in seven additional peer reviewed publications over the last year (two refereed conference papers and 5 journal papers). The work furthermore resulted in 14 conference presentations at regional, national, and international conferences and scientific meetings. Four Master's thesis were submitted over the reporting period.

Published Journal and Conference Publications from September 2018-December-2019:

1. James N. Talbert, Samuel R. Cantrell, Md. Abdul Ahad Talukder, Luisa M. Scolfaro, Wilhelmus J. Geerts, "Electrical Characterization of Silicon – Nickel Iron Oxide Heterojunctions", MRS Advances 4 (2019) 2241-2248, DOI: 10.1557/adv.2019.321
2. Binod D.C., Andres Oliva, Anival Ayala, Shankar Acharya, Fidele Twagirayezu, James Nick Talbert, Luisa M. Scolfaro, Wilhelmus J. Geerts, "Magnetic Properties of reactive co-sputtered NiFe-oxide samples", IEEE Trans. on Magn. 55 (2019) 2900205, pp. 2900205-1-6, DOI: 10.1109/TMAG.2018.2866788.
3. Shankar Acharya, Brian Collier, Wilhelmus Geerts, "Dual Beam Modulated Magneto-Optical Measurement Setup", accepted for publication in Rev. Sc. Instrum., Nov. 2019.
4. John Petersen, Luisa M. Scolfaro, Pablo D. Borges, Wilhelmus J. Geerts, "Symmetry consideration on band filling and first optical transition in NiO", Eur. Phys. J. B (2019): 92:232, https://doi.org/10.1140/epjb/e2019-100363-5.
5. James Shook, Pablo D. Borges, Luisa M. Scolfaro, Wilhelmus J. Geerts, "Effects of vacancies and p-doping on the optoelectronic properties of Cu- and Ag-based transparent conducting oxides", J. Appl. Phys. 126 (2019) 075702.
6. James Shook, Luisa M. Scolfaro, Pablo D. Borges, Wilhelmus J. Geerts, "Structural stability and electronic properties of XTO2 (X=Cu, Ag; T=Al, Cr): An ab initio study including X vacancies and Mg doping", Solid State Sciences 88 (2019) pp. 48-56.
7. Fidele J. Twagirayezu, Md. Abdul Ahad Talukder, Wilhelmus J. Geerts, "Magnetic Properties of RF sputtered NiO and Ni0.8Fe0.2O1-? samples grown on SiO2/Si substrates", Materials Research Innovations, (2018) pp 1-8, DOI: 10.1080/14328917.2018.1558797.

Presentations and posters at conferences from September 2018-December-2019:

8. Samuel R Cantrell, Luisa Scolfaro, Pablo Borges, Wilhelmus J. Geerts, GGA+U and hybrid functional calculations of intrinsic defects and transition metal doping in NiO, oral presentation at APS April meeting in Denver Colorado, April 13-16, 2019.
9. James Nick Talbert, Wilhelmus J. Geerts, Luisa Scolfaro, "Electrical Characterization of Nickel oxide and Nickel Iron Oxide Thin Films and Resistive Random Access Memory Devices grown by Radio Frequency Sputtering", Fall-2018 TSAPS oral presentation, October 15, Houston.
10. Sam Cantrell, Luisa Scolfaro, Pablo Borges, Wilhelmus Geerts, "Copper-induced features in rocksalt NiO using ab initio calculations", Fall-2018 TSAPS oral presentation, October 15, Houston.
11. Kolton Dieckow, Sarah Beth Ragan, Chandan Howlader, Binod D.C., Wilhelmus Geerts, "Biaxial VSM Sensitivity and Crosstalk Measurement Dependence for Sxx(x,y,z), Sxy(x,y,z), and Sxz(x,y,z)", poster presentation 2019-Fall meeting of the TSAPS, Lubbock, October 25-26 2019.
12. Nick Talbert, Wilhelmus J. Geerts, "Electrical Characterization of Silicon Nickel Iron Oxide heterojunctions", poster presentation at MRS Spring meeting Spring 2019, April 22-26, Phoenix.
13. Samuel Zamora, Wilhelmus Geerts, Joselyn Lesikar, Binod, D.C., "Measuring the Magnetic Properties of 3D Printed Materials Using the Vibrating Sample Magnetometer", TSAP spring meeting 2019, Tarleton State University, March 8, 2019.
14. Binod D.C., Luisa Scolfaro, Wilhelmus J. Geerts, "Pole Figure Measurements on RF-Sputtered Ni0.8Fe0.2-Thin Films", TSAP spring meeting 2019, Tarleton State University, March 8, 2019.
15. Rigoberto Mayorga-Luna, Chandler Hutton, Wilhelmus J. Geerts, "Algorithm to Diagnose Problematic Wires or Contacts of Four Point Probe Measurement Setup", Wise conference March 8, 2019, Texas State University.
16. Selena Rose Najar, Joselyn Lesikar, Binod D.C., Luisa Scolfaro, Wilhelmus J. Geerts, "Studying the Temperature Dependent Magnetic Properties of Reactive RF Co-sputtered NiFeO Thin Films Using VSM", Wise conference March 8, 2019, Texas State University.
17. Shankar Acharya, Luisa Scolfaro, Wilhelmus J. Geerts, "Dual Beam Detection Technique to Study MOKE", Wise conference March 8, 2019, Texas State University.
18. Samuel Cantrell, Luisa Scolfaro, Wilhelmus J. Geerts, "Stability of transition metal impurities in nickel oxide via formation energy calculations, Wise conference March 8, 2019, Texas State University.
19. Selena Rose Najar, Joselyn Lesikar, Binod D.C., Luisa Scolfaro, Wilhelmus J. Geerts, "Temperature Dependence of the Magnetic Properties of Reactive RF Sputtered NiFeO Thin Films", Fall-2018 TSAPS

presentation, October 15, Houston.
20. Noel Gamez, Wilhelmus Geerts, Luisa Scolfaro, William Spencer, Giri Joshi, “Iron Gallium Magnetostriction Measurement Setup”, Fall-2018 TSAPS presentation, October 15, Houston.
21. Selena Rose Najar, Joselyn Lesikar, Binod D.C., Luisa Scolfaro, Wilhelmus Geerts, “Preliminary Temperature Dependence of the Magnetic Properties of Reactive RF Sputtered NiFeO Thin Films”, Symposium for Undergraduate Research Exploration 2018, University of Texas at Austin, October 4, 2018.
22. N. Gamez, W. Spencer, G. Joshi, L. Scolfaro, W. Geerts, “Iron Gallium Magnetostriction Measurement Setup”, Symposium for Undergraduate Research Exploration 2018, University of Texas at Austin, October 4, 2018.
23. Clint Boldt, Md. Abdul Ahad Talukder, James Nick Talbert, Luisa Scolfaro, Wilhelmus J. Geerts, ”Properties of carrier traps in diode and RRAM devices via DLTS”, Fall-2018 TSAPS presentation, October 15, Houston.

Thesis and Dissertations:
1. Shankar Acharya, “Dual Beam Detection Technique to Study Magneto-Optical Kerr effect”, thesis Texas State University, San Marcos, May 2019.
2. Nick Talbert, “Electrical Characterization of Nickel Oxide and Nickel Iron Oxide thin films and resistive random access memory devices grown by Radio Frequency Sputtering”, thesis TxState University, San Marcos, Dec. 2019.
3. Binod D.C., “The Magnetic Characterization of Permalloy and Permalloy Oxide Grown by RF Magnetron Sputtering”, thesis Texas State University, San Marcos, December 2019.
4. Sam Cantrell, “Optoelectronic Properties and Energetics of Defects and Impurities in NiO studied using Ab Initio Calculations”, thesis Texas State University, December 2019.

Honors and Awards: Honors and Awards:
[1] Wim Geerts (PI) and Luisa Scolfaro (co-PI), “Optical and Electrical Properties of NiFe-oxide Thin Films” (67340-MS-REP), Army Research Office, Research and Education Program for Historically Black Colleges and Universities and Minority-Serving Institutions (HBCU/MI), $387,691.- (09/2015-09/2019).
[2] Wim Geerts (PI), Chris Rhodes, Maggie Chen, Ravi Droopad, Nikoleta Theodoropoulou, “MRI: Vibrating Magnetometer for Materials Research and Education”, NSF MRI acquisition proposal, ($321,900), September 15 2017 through August 31 2020.
[3] PI on URAP/HSAP -2018 request in support of Optical and Electrical Characterization of NiFe-oxide thin films Research, PI together with Dr. Luisa Scolfaro (Army Research Office) ($7,500), summer 2019, accepted, with award contingent on the availability of funds.
[4] Graduate students Sam Cantrell, Binod D.C, and James Shook who all three worked on the grant were recognized in May 2019 by the Physics department for academic excellence. This is an award that recognizes graduate students that maintain a GPA of 3.75 or higher.
[5] Graduate student Shankar Acharya received the outstanding graduate Laboratory Instructor award from the department of Physics in May 2019.
[6] Graduate student James Shook received the excellence in Graduate Research award in Spring 2019.
[7] Undergraduate student Sam Zamora received the excellence in Introductory Physics award in May 2019.

Protocol Activity Status:

Technology Transfer: The thesis work of Binod D.C. let to a new method to align samples in a vibrating sample magnetometer. We are currently in the process of disclosing this invention to the University. The invention disclosure will be submitted in December 2019.

PARTICIPANTS:

Participant Type: Co PD/PI
Participant: Luisa Scolfaro
Person Months Worked: 2.00 **Funding Support:**
Project Contribution:
International Collaboration:
International Travel:
National Academy Member: N
Other Collaborators:

Participant Type: PD/PI

RPPR Final Report
as of 03-Jan-2020

Participant: Wilhelmus Geerts
Person Months Worked: 4.00 **Funding Support:**
Project Contribution:
International Collaboration:
International Travel:
National Academy Member: N
Other Collaborators:

Participant Type: Graduate Student (research assistant)
Participant: Shankar Acharya
Person Months Worked: 9.00 **Funding Support:**
Project Contribution:
International Collaboration:
International Travel:
National Academy Member: N
Other Collaborators:

Participant Type: Graduate Student (research assistant)
Participant: Binod D.C.
Person Months Worked: 12.00 **Funding Support:**
Project Contribution:
International Collaboration:
International Travel:
National Academy Member: N
Other Collaborators:

Participant Type: Graduate Student (research assistant)
Participant: James Nick Talbert
Person Months Worked: 9.00 **Funding Support:**
Project Contribution:
International Collaboration:
International Travel:
National Academy Member: N
Other Collaborators:

Participant Type: Graduate Student (research assistant)
Participant: Sam Cantrell
Person Months Worked: 12.00 **Funding Support:**
Project Contribution:
International Collaboration:
International Travel:
National Academy Member: N
Other Collaborators:

Participant Type: Graduate Student (research assistant)
Participant: Md Ahad Abdul Talukder
Person Months Worked: 1.00 **Funding Support:**
Project Contribution:
International Collaboration:
International Travel:
National Academy Member: N
Other Collaborators:

RPPR Final Report
as of 03-Jan-2020

Participant Type: Graduate Student (research assistant)
Participant: Kolton Dieckow
Person Months Worked: 1.00 **Funding Support:**
Project Contribution:
International Collaboration:
International Travel:
National Academy Member: N
Other Collaborators:

Participant Type: Undergraduate Student
Participant: Lauren Trombley
Person Months Worked: 2.00 **Funding Support:**
Project Contribution:
International Collaboration:
International Travel:
National Academy Member: N
Other Collaborators:

Participant Type: High School Student
Participant: Sarah-Beth Ragan
Person Months Worked: 2.00 **Funding Support:**
Project Contribution:
International Collaboration:
International Travel:
National Academy Member: N
Other Collaborators:

Participant Type: Undergraduate Student
Participant: Rigoberto Mayorga-Luna
Person Months Worked: 1.00 **Funding Support:**
Project Contribution:
International Collaboration:
International Travel:
National Academy Member: N
Other Collaborators:

Participant Type: Undergraduate Student
Participant: Clint Boldt
Person Months Worked: 1.00 **Funding Support:**
Project Contribution:
International Collaboration:
International Travel:
National Academy Member: N
Other Collaborators:

Participant Type: Undergraduate Student
Participant: Noel Gamez
Person Months Worked: 1.00 **Funding Support:**
Project Contribution:
International Collaboration:
International Travel:
National Academy Member: N
Other Collaborators:

RPPR Final Report
as of 03-Jan-2020

Participant Type: Undergraduate Student
Participant: Salamon Gallegos
Person Months Worked: 2.00 **Funding Support:**
Project Contribution:
International Collaboration:
International Travel:
National Academy Member: N
Other Collaborators:

Participant Type: Undergraduate Student
Participant: Selena Rose Najar
Person Months Worked: 1.00 **Funding Support:**
Project Contribution:
International Collaboration:
International Travel:
National Academy Member: N
Other Collaborators:

Participant Type: Undergraduate Student
Participant: Sam Zamora
Person Months Worked: 1.00 **Funding Support:**
Project Contribution:
International Collaboration:
International Travel:
National Academy Member: N
Other Collaborators:

CONFERENCE PAPERS:

Publication Type: Conference Paper or Presentation **Publication Status:** 1-Published
Conference Name: 2016 MRS Spring Meeting
Date Received: 01-Sep-2016 Conference Date: 29-Mar-2016 Date Published: 02-Jun-2016
Conference Location: Phoenix, Arizona
Paper Title: Ab initio study of oxygen vacancy effects on electronics and optical properties of NiO
Authors: John Petersen, Fidele Twagirayezu, Pablo D. Borges, Luisa Scolfaro, Wilhelmus Geerts
Acknowledged Federal Support: **Y**

Publication Type: Conference Paper or Presentation **Publication Status:** 1-Published
Conference Name: 2016 MRS Spring Meeting
Date Received: 01-Sep-2016 Conference Date: 28-Mar-2016 Date Published: 26-Aug-2016
Conference Location: Phoenix Arizona
Paper Title: FTIR Ellipsometry study on RF sputtered Permalloy-oxide Thin Films
Authors: Md. Abdul Ahad Talukder, Yubo Cui, Maclyn Compton, Luisa Scolfaro, Stefan Zollner, Wilhelmus Geerts
Acknowledged Federal Support: **Y**

RPPR Final Report
as of 03-Jan-2020

Publication Type: Conference Paper or Presentation **Publication Status:** 1-Published
Conference Name: MMM conference
Date Received: 01-Sep-2017 Conference Date: 04-Oct-2016 Date Published: 07-Feb-2017
Conference Location: Lousiana
Paper Title: Electronics and Optical properties of antiferromagnetic Iron doped NiO – A first principles study
Authors: John E. Petersen, Fidele Twagirayezu, Luisa M. Scolfaro, Pablo D. Borges, Wilhelmus J. Geerts
Acknowledged Federal Support: **Y**

Publication Type: Conference Paper or Presentation **Publication Status:** 1-Published
Conference Name: MMM conference
Date Received: 01-Sep-2017 Conference Date: 04-Oct-2016 Date Published: 06-Feb-2017
Conference Location: Lousiana
Paper Title: Tilt angle dependence of the modulated interference effect in Photo-elastic Modulators
Authors: Md. Abdul Ahad Talukder, Wilhelmus J. Geerts
Acknowledged Federal Support: **Y**

Publication Type: Conference Paper or Presentation **Publication Status:** 1-Published
Conference Name: International Conference on Magnetism
Date Received: 10-Sep-2019 Conference Date: 18-Jul-2018 Date Published: 15-Aug-2018
Conference Location: San Francisco
Paper Title: Dual Beam MOKE Detection to Suppress the Effect of Modulated Interference Effects i
Authors: Shankar Acharya, Brian Collier, Abdul Ahad Talukder, Wilhelmus J. Geerts
Acknowledged Federal Support: **Y**

Publication Type: Conference Paper or Presentation **Publication Status:** 1-Published
Conference Name: MRS Spring Meeting
Date Received: 17-Dec-2019 Conference Date: 24-Apr-2019 Date Published: 20-Jul-2019
Conference Location: Phoenix
Paper Title: Electrical Characterization of Silicon – Nickel Iron Oxide Heterojunctions
Authors: James, Talbert, Samuel Cantrell, Md, Abdul Ahad Talukder, Luisa, Scolfaro, Wilhlemus Geerts
Acknowledged Federal Support: **Y**

DISSERTATIONS:

Publication Type: Thesis or Dissertation
Institution: Texas State University at San Marcos
Date Received: 01-Sep-2016 Completion Date: 7/16/16 1:47AM
Title: Electrical and Optical Properties of RRAM, Thesis Yubo Cui
Authors: Yubo, Cui
Acknowledged Federal Support: **Y**

Publication Type: Thesis or Dissertation
Institution: Texas State University at San Marcos
Date Received: 01-Sep-2017 Completion Date: 7/27/17 10:03AM
Title: Theoretical and Experimental study of the Optical Properties of Fe doped Nickel oxides
Authors: Fidele Twagirayezu
Acknowledged Federal Support: **Y**

RPPR Final Report
as of 03-Jan-2020

Publication Type: Thesis or Dissertation
Institution: Texas State University San Marcos
Date Received: 03-Sep-2018 Completion Date: 11/29/17 4:29AM
Title: IMPURITIES IN ANTIFERROMAGNETIC TRANSITION-METAL OXIDES – SYMMETRY AND OPTICAL TRANSITIONS
Authors: John Emil Petersen III
Acknowledged Federal Support: **Y**

Publication Type: Thesis or Dissertation
Institution: Texas State University
Date Received: 03-Sep-2018 Completion Date: 7/19/18 5:00AM
Title: FIRST PRINCIPLES STUDY ON THE EFFECTS OF VACANCIES AND Mg DOPING ON THE PHYSICAL PROPERTIES OF CuAlO2, AgAlO2, CuCrO2, AND AgCrO2 TRANSPARENT CONDUCTOR OXIDES
Authors: James A. Shook
Acknowledged Federal Support: **N**

Publication Type: Thesis or Dissertation
Institution: Texas State University
Date Received: 03-Sep-2018 Completion Date: 12/1/17 6:00AM
Title: INFLUENCE OF OXYGEN FLOW ON THE MICROSTRUCTURE, RESISTIVITY, AND FARADAY ROTATION OF REACTIVE RF SPUTTERED NIO AND FE-DOPED NIO THIN FILMS.
Authors: Md Abdul Ahad Talukder
Acknowledged Federal Support: **Y**

Publication Type: Thesis or Dissertation
Institution: Texas State University San Marcos
Date Received: 10-Sep-2019 Completion Date: 5/16/19 2:58AM
Title: Dual Beam Detection Technique to Study Magneto-Optical Kerr effect
Authors: Shankar Acharya
Acknowledged Federal Support: **Y**

Publication Type: Thesis or Dissertation
Institution: Texas State University at San Marocs
Date Received: 16-Dec-2019 Completion Date: 12/8/19 12:00PM
Title: Electrical Characterization of Nickel Oxide and Nickel Iron Oxide thin films and resistive random access memory devices grown by Radio Frequency Sputtering
Authors: James Nick Talbert
Acknowledged Federal Support: **Y**

Publication Type: Thesis or Dissertation
Institution: Texas State University at San Marcos
Date Received: 16-Dec-2019 Completion Date: 12/8/19 6:00AM
Title: Optoelectronic Properties and Energetics of Defects and Impurities in NiO studied using Ab Initio Calculations
Authors: Sam Cantrell
Acknowledged Federal Support: **Y**

RPPR Final Report
as of 03-Jan-2020

Final Progress Report

Contract No. W911NF-15-1-0394

Grant number: 67340-ARO-MS-REP

"Optical and Electrical Properties of NiFe-oxide Thin Films"

ARO GOR:

Dr. Evan Runnerstrom
Evan.l.runnerstrom.civ@mail.mil
919-549-4259
US ARMY ACC-APG-RTP W911NF
800 PARK OFFICE DRIVE
SUITE 4229
RESEARCH TRIANGLE PARK NC 27709

Date submitted: 16 December 2019
P.I.: Dr. Ir. Wilhelmus J. Geerts
Texas State University
601 University Drive
San Marcos, TX 78666
wjgeerts@txstate.edu
Tel: 512-245-1821

REPORT DOCUMENTATION PAGE

Form Approved
OMB No. 0704-0188

1. REPORT DATE *(DD-MM-YYYY)*	**2. REPORT TYPE**	**3. DATES COVERED** *(From - To)*
30-11-2019	Final Progress Report	09/01/2015- 08/31/2019

4. TITLE AND SUBTITLE

Title: Optical and Electrical Properties of NiFe-oxide Thin Films

5a. CONTRACT NUMBER
W911NF-15-1-0394

5b. GRANT NUMBER
67340-ARO MS-REP

5c. PROGRAM ELEMENT NUMBER

6. AUTHOR(S)

Wilhelmus J. Geerts, Luisa Scolfaro

5d. PROJECT NUMBER

5e. TASK NUMBER

5f. WORK UNIT NUMBER

7. PERFORMING ORGANIZATION NAME(S) AND ADDRESS(ES)

Department of Physics
Texas State University
601 University Drive
San Marcos, TX 78666

8. PERFORMING ORGANIZATION REPORT NUMBER

9. SPONSORING / MONITORING AGENCY NAME(S) AND ADDRESS(ES)
US ARMY ACC-APG-RTP W911NF
SUITE 4229

Attn: Evan L. Runnerstrom

10. SPONSOR/MONITOR'S ACRONYM(S)

11. SPONSOR/MONITOR'S REPORT NUMBER(S)

12. DISTRIBUTION / AVAILABILITY STATEMENT

DISTRIBUTION STATEMENT A: For public release

13. SUPPLEMENTARY NOTES

14. ABSTRACT: The optical, electrical, magnetic, and structural properties of reactive RF sputtered Fe-doped NiO thin films were investigated by experimental and computational methods for possible application in novel memory devices. Magnetic, optical, and Xray measurement data confirm that RF sputtered thin films have the NiFe-oxide rocksalt crystal structure with a (111) texture and small crystallites. The materials properties depend on oxygen or metal vacancy concentration which can be modified by adjusting deposition parameters including oxygen partial pressures, Ar pressure, and sputter power. Determined materials properties include saturation magnetization 1-2 emu/cm^3, refraction index 2.2-2.4, mobility, dielectric constant 300-10, resistivity 10^3-10^8 Ohm cm, mobility 0.8-8 10^{-3} cm^2/Vs. $Ni_{0.8}Fe_{0.2}O$ containing metal vacancies are most conductive and when sputtered on n-Si form strongly rectifying heterojunctions. Rf sputtered $Ni_{0.8}Fe_{0.2}O$ are stable up to temperatures of 500°C but becomes ferromagnetic when annealed at higher temperatures. Type 1 resistive switching was observed in RRAM devices employing NiFeO.

15. SUBJECT TERMS
Final Progress Report, transition metal oxides, optical properties, charge transport, magnetic properties, RRAM, electron blockers, rectifying heterojunctions.

16. SECURITY CLASSIFICATION OF:			**17. LIMITATION OF ABSTRACT**	**18. NUMBER OF PAGES**	**19a. NAME OF RESPONSIBLE PERSON**
a. REPORT	**b. ABSTRACT**	**c. THIS PAGE**			Wilhelmus J. Geerts
U	U	U	SAR	32	**19b. TELEPHONE NUMBER** *(include area code)* 512-245-1821

Standard Form 298 (Rev. 8-98)
Prescribed by ANSI Std. Z39.18

Foreword

This Final report summarizes the most important conclusions that came out of the ARO sponsored project “Optical and Electrical Properties of NiFeO Thin Films” conducted at Texas State University from September 2015 to September 2019 in the research groups of Drs. Luisa Scolfaro and Wim Geerts. The samples were prepared in the Orion 8 AJA sputter system of the Nanofabrication Research Service Center (class 1000 cleanroom) at Texas State University. The AJA sputter system is also used by other users including class projects, research groups of other faculties within the Physics department, and external users sputtering a variety of materials including ITO, Ag, Zn, Co, Al, Cu, Ti, and Ta. The AJA system has a background pressure in the 10^{-8} Torr range. All experiments except for the RBS and XPS measurements were performed using equipment available from the Analysis and Research Service Center at Texas State University and equipment available from the Optical Characterization Lab. All calculations were performed using the TxState computer cluster. All experiments and calculations were performed by undergraduate, MSc., PhD., and high school students working together with the PIs, Drs. Scolfaro and Geerts. No postdoc and technicians were used for the project. The work resulted in 12 peer reviewed journal and conference papers, 25 oral conference presentations and 16 poster presentations all but one with a student first authors. Thirty-eight students contributed to the project. The most important conclusions from the project are summarized in this report. The project would not have been possible without the direct financial support of DOD via grant W911NF-15-1-0394. In addition, the project benefited from two DOD instrumentation grants (electrical characterization: W911NF-16-R-0024, Scanning probe: 68869-RT-REP), an NSF-MRI grant (MRI: Vibrating Magnetometer for Materials Research and Education 1726970), and financial and in-kind support from Texas State (travel funds, and research enhancement grant).

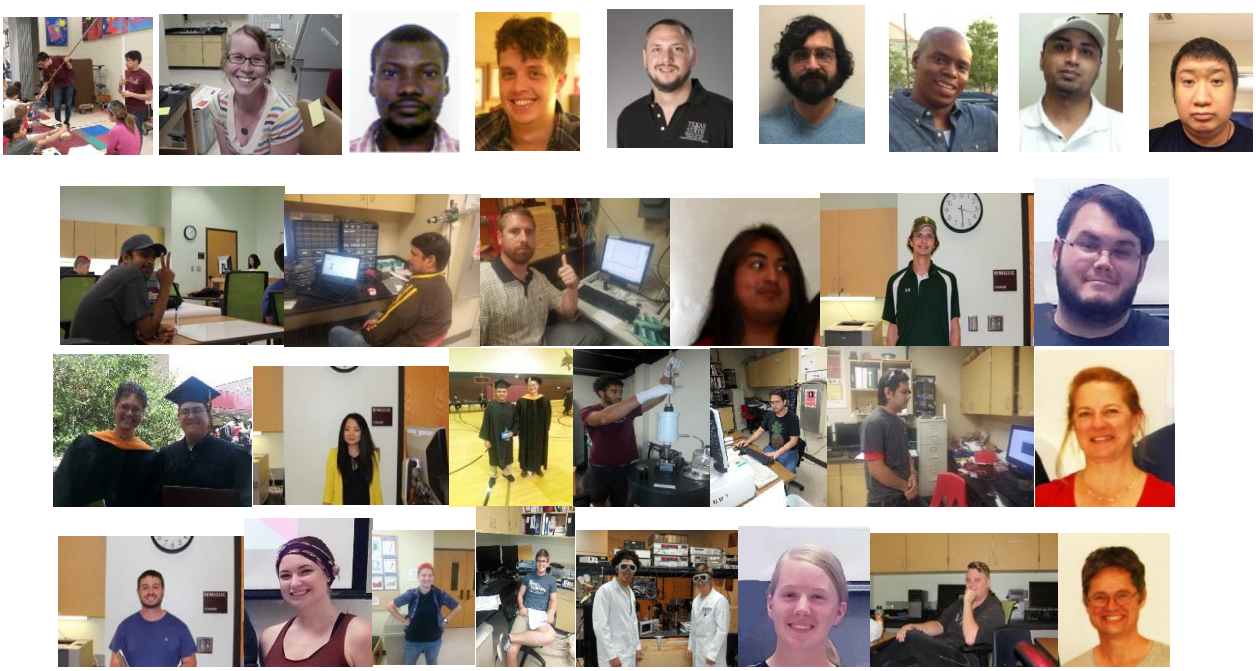

TABLE OF CONTENTS

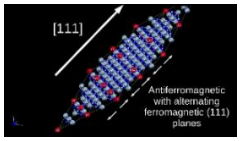

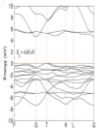

Statement of the problem studied:

The objective of this research project was to conduct fundamental research to better understand electronic transport in RF sputtered Fe doped nickel oxide thin films for application in radiation-hard, low-energy, high-speed logic resistive-memory devices. A complementary experimental and theoretical approach was followed to investigate the optical and electrical transport properties of RF sputtered NiFe-oxide thin films and their applicability to RRAM devices.

Experimental goals:

(1) structural and chemical characterization using XRD, EDAX, XPS and RBS.

(2) optical characterization using FTIR, ellipsometry, and optical transmission measurements.

(3) electrical characterization including four and two-point probe IV measurements, CV measurements, and DLTS measurements. Samples are continuous thin films and devices. Experiments are supplemented by device computations using the finite element technique.

(4) magnetic characterization using VSM, Magneto-Optical Kerr magnetometry, and MFM.

Theoretical goals:

DFT calculations to better understand the electronic structure and ion mobility of NiO and doped NiO. In particularly the effect of iron-doping and vacancies on the optical, magnetic, and electrical properties.

Summary of the most important results:

1. **Crystal Structure:** XRD measurements show that reactive RF sputtered $Ni_{0.8}Fe_{0.2}O$ deposited at sputter pressures between 1E-4<p<0.8E-2 Torr and substrate temperature between RT and 600 Celsius has the rocksalt crystal structure. FTIR measurements performed on thin film samples sputtered on microscope slides or silicon wafers show a single phonon peak in the far infrared consistent with the rocksalt crystal structure [1]. This is in sharp contrast with the known atmospheric pressure phase diagram of NiFeO which shows a solubility of less than 2% at RT [2]. RF sputtered thin films of NiFeO have a (111) texture under both low or high oxygen flow conditions. This is different from RF sputtered NiO films whose texture depends on the oxygen flow during deposition [3,4,5]. The crystallinity of the RF sputtered NiFeO films appears to depend on sputter pressure, substrate temperature, substrate, Fe concentration, sample-holder rotation speed, film thickness, and oxygen flow [6,7,8]. Typical crystal size as determined from the width of diffraction peaks is 25% smaller for NiFeO compared to NiO films sputtered under similar conditions [6]. This is consistent with literature which shows that doping of NiO with other elements, in general, will reduce the crystal size [9,10].

2. **Sputter Process optimization:** EDAX measurements show that the atomic concentration ratio of Ni and Fe in reactive RF sputtered NiFeO samples is the same as that of the used target materials when the targets were pre-sputtered for 2 minutes prior to each deposition run. Our results furthermore indicate that the homogeneity of the flux ratio of oxygen to metal atoms arriving at the substrate affects the electrical properties of the sputtered NiFeO material (see also results presented in section 3). To realize a well-defined oxide layer that is homogeneous across a wafer the sputter system was modified and the sputter process parameters were chosen as follows:

a. A substrate shutter was installed in the sputter chamber to reduce the metal atom flux transient at the start of the deposition process. With the modified setup it is possible to open the sputter gun shutters and allow an oxide to be formed on the targets prior to starting the deposition on the substrate by opening the substrate shutter. It is suspected that without a substrate shutter the seed layer of the transition metal oxide has a lower oxygen concentration than the bulk section of the thin film.
b. The sputter pressure was increased from <1 mTorr to 8 mTorr. This increased pressure reduced the mean free path of the sputtered atoms and widened the sputter beam resulting in a more homogeneous flux of metal atoms arriving at the substrate.
c. Co-deposition using two sputter guns on opposite sides of the substrate holder was used to further reduce the variation of the metal sputter flux across the substrate holder.
d. For each deposition run, we mounted the substrate exactly in the center of the substrate-holder. Using funds of the grant, a sampleholder dedicated to NiFeO depositions was purchased to avoid possible cross-contamination by re-sputtering of materials used by other users of the AJA sputtering system.

Furthermore, it should be mentioned that for all sputter runs done during the project the substrate was rotated during deposition, further improving the homogeneity of the oxide properties across the device wafers. Not rotating the substrate during deposition also impacts the texture and crystallinity of the films [7].

Only after above mentioned changes were implemented the scattering of the electrical properties across experiments reduced sufficiently to be able to recognize patterns and make meaningful

correlations between electrical properties and deposition parameters. The importance of a constant deposition flux (both metal and oxygen) across the substrate is explained by the strong dependence of the resistivity on the oxygen % in the sputter gas: the resistivity of NiFeO changes with five orders of magnitude when changing the oxygen flow during deposition with a factor 10. See also the data presented in section 3.

3. **Stoichiometry of the oxide films and 4pp resistivity:** The stoichiometry of NiFeO films and with it the electrical properties strongly depend on the partial oxygen pressure during deposition, the total sputter pressure during deposition, the sputter power, and the number of guns used during deposition. The main factor that determines the stoichiometry of the samples is the ratio of the metal to oxygen flux arriving at the substrate. The incident metal flux and its distribution across the substrate can be modified by the sputter power, the number of sputter guns, the sputter pressure, and or the oxygen partial pressure. The effect of oxygen partial pressure on the metal sputter rate is by the presence or absence of an oxide scale on the surface of the targets. The formation of a permanent oxide layer on the target's surfaces will reduce the sputter rate. Figure 1 below shows the sputter rate as a function of the oxygen partial pressure at 8 mTorr using two guns at 200 Watt each.

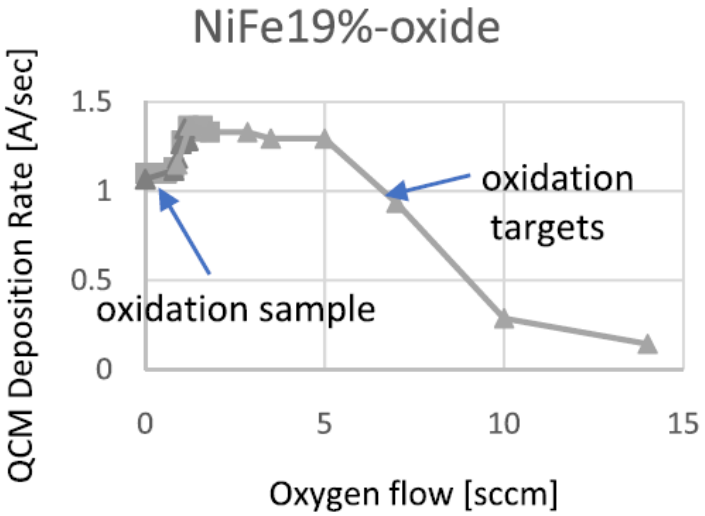

Fig. 1. Deposition rate versus oxygen flow for two guns at 8 mTorr [11].

Over the course of the project, three different methods were used to determine the stoichiometry of the NiO and NiFeO films directly (EDAX, RBS, XPS). The results of each method were compared with the resistivity-oxygen flow plots measured by linear 4pp measurements on films sputtered on insulating substrates including microscope slides and quartz coupons:

a. Edax: Early on in the project graduate student Yubo Cui used EDAX [12] to estimate the oxygen to metal ratio of the sputtered NiFeO films. The EDAX spectra were measured at different electron beam acceleration voltages. The McXRayLite software package developed by Prof. Guavin [13,14,15] was used to model the generation and collection of Xray photons in the multilayer samples. Parameters including film thicknesses and chemical composition were adjusted in the model until the simulated and measured EDAX spectra were similar. Four samples deposited at low sputter pressure (1 mTorr) were analyzed this way and all showed a large

concentration of oxygen vacancies, i.e. up to half of the oxygen atoms seemed to be missing. The determined oxygen vacancy concentrations were smaller for samples sputtered at higher oxygen flow. It is suspected that absorption of the low energy Xray photons originating from the oxygen atoms by oil on the detector window is the main spoiler and underestimates the oxygen concentration with this method. Note that for sputter pressures below 1 mTorr the partial oxygen pressure is too low to result in a permanent oxide scale on the targets. So metallic atoms are sputtered in this mode and oxidation happens mainly on the substrate. Th sputter rate hardly depends on oxygen flow and the resistivity-oxygen flow chart is monotonous increasing (see Fig. 2 below) [12].

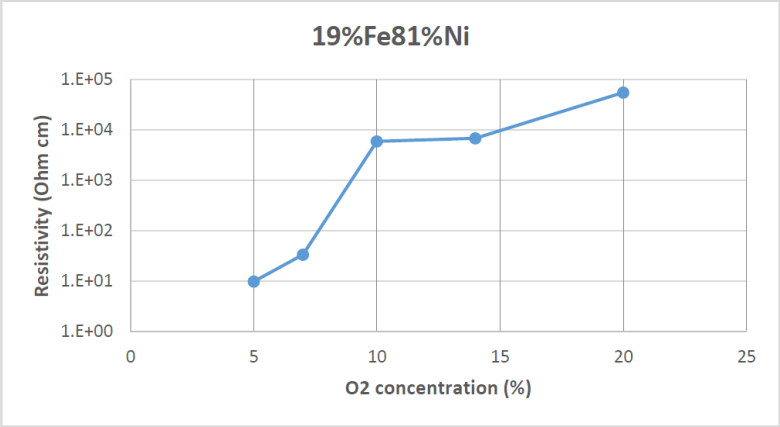

Fig.2 Resistivity as a function of O_2 concentration in sputter gas for PyO for a total sputter pressure of 1 mTorr (single gun, 240 Watt) [12].

b. RBS: RBS analysis was done by Evans Analytical on two thick RF sputtered NiO samples sputtered at 8 mTorr. Note that at these pressures an oxide scale will develop on the targets above 5% oxygen content in the sputter gas (see also Fig. 1 above). The RBS results show that the samples sputtered a low oxygen flow (1% O_2 in the sputter gas) has an oxygen vacancy concentration of 11+/-6% and the sample sputtered at high oxygen flow (with 10% O_2 in the sputter gas) has a nickel vacancy concentration of 23+/-6% [6]. The resistivity of NiO films sputtered at 8 mTorr as a function of the oxygen concentration in the sputter gas is shown in Fig. 3 below [6,18]. We expect that the peak is close to stoichiometric composition. DFT calculations done by John Peterson show that only at very high oxygen vacancy concentration, oxygen vacancies are expected to be donors [17]. The decrease of the resistivity above 10% is due to metal vacancies that act like acceptors in NiO. To explain the decrease of the resistivity for oxygen flows below 10% two explanation were further tested (1) n-doping by oxygen vacancies; (2) incomplete oxidation of part of the Ni caused by deposition inhomogeneities. DFT calculations done by PhD student John Peterson showed that only at very high oxygen vacancies oxygen will act as a donor so the n-doping hypothesis was rejected. The 2nd hypothesis was tested by modifying the deposition geometry (see section 2 above) in the chamber and indeed changed the resistivity versus oxygen flow for the lower oxygen flow rates (see section 3c below).

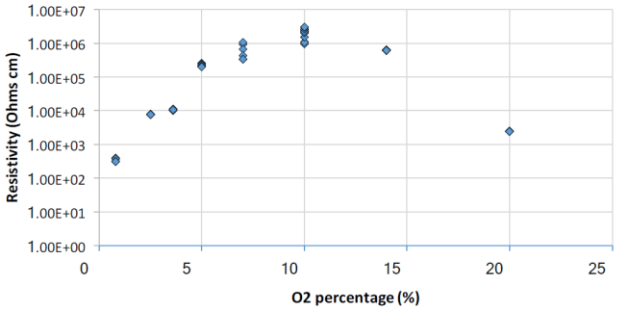

Fig. 3. Resistivity versus oxygen concentration in sputter gas for RF sputtered NiO films sputtered at 8 mTorr (one gun 240 Watt) [18].

c. XPS: In order to get a qualitative understanding of the relation between O_2 percentage in the sputter gas and the oxygen content in the NiFeO films XPS measurements were done on two oxygen flow series [6, 7, 11]. The first attempt was done by graduate student Ahad Talukder using the XPS system on the TxState MBE cluster. Samples were sputtered with a single gun at 8 mTorr and not capped on 1"^{2} quartz coupons. After exposure, the samples were loaded in the XPS system and annealed to 150 ^oC for one hour. No correlation was found between the oxygen flow during deposition and the Ni-XPS spectra. The 2nd attempt was done by graduate student Binod D.C. in collaboration with Dr. Tim Hossain of Cerium Labs. The measurements were done using the XPS system of Cerium Labs in Austin. Their XPS instrument contains a sputter gun, so it is possible to clean the sample's surface after loading it in the vacuum chamber. XPS measurements were done on NiFeO samples co-sputtered at 8 mTorr/200 Watt (after optimization of sputtering geometry lined out in section 2 above). All samples were capped with an Au or Pt cap layer before they were taken out of the sputter system. After loading the sample in the XPS system part of this cap layer, but not all, was removed, before taking the XPS spectra. A strong correlation was found between the oxygen flow during deposition and the Ni-XPS spectra. For films sputtered at or below 10% oxygen in the sputter gas, part of the Ni in the NiFeO films is still metallic [7,11].

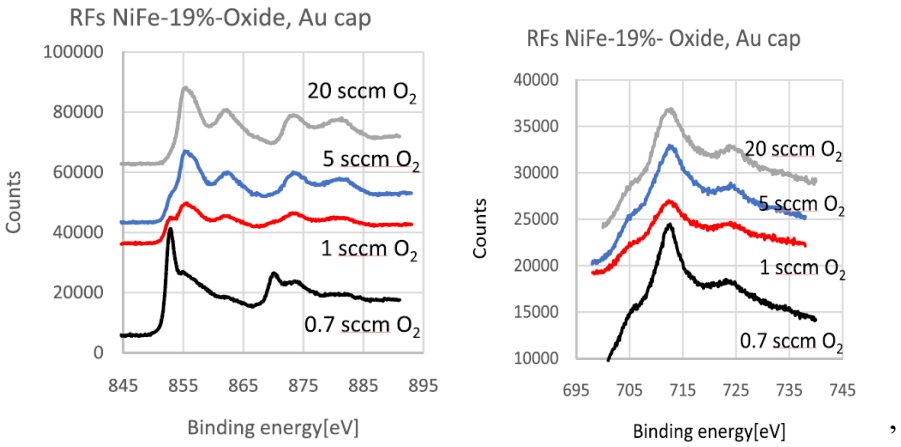

Fig. 4. XPS spectra of RF sputtered NiFeO (8 mTorr, co-sputtering, 200 Watt per gun) for different oxygen flow (a) Ni peaks (left) showing the existence of metallic Ni for films RF sputtered films (8 mTorr) using 10% or less oxygen in the sputter gas (b) Fe peaks that are all oxidized (right) [7, 11].

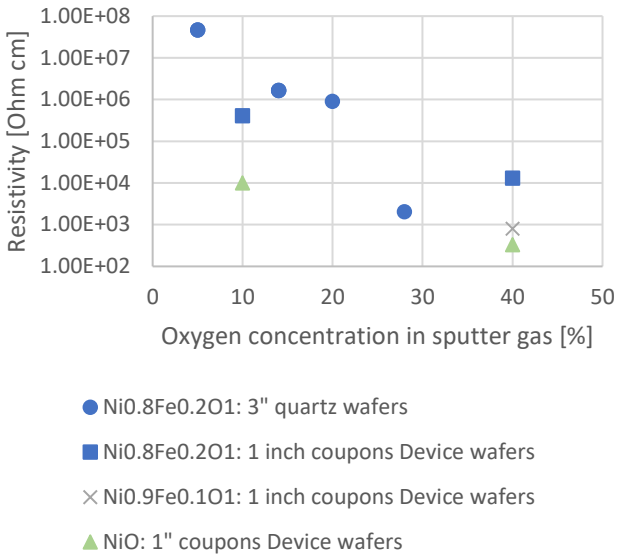

Fig. 5 resistivity versus oxygen flow graph for NiFeO films for thin film co-sputtered on at 8 mTorr, two guns each 200 Watt power.

Figure 5 above shows the oxygen flow dependence of the resistivity of samples without cap-layer co-sputtered at 8 mTorr/200 Watt (deposited after process revisions described in section 2). No maximum of the resistivity was observed within the investigated sputter gas oxygen concentration range. Note that these measurements were done on 3" diameter quartz wafers so also the shading effects of the clips holding the substrate on the substrate-holder was strongly reduced. The maximum of the resistivity versus oxygen flows as observed when depositing with a single gun is not reproduced when co-sputtering. We believe that this is due to the inhomogeneous metal flux rate at the substrate when sputtering with a single gun. Similar results as shown in Fig. 5 were obtained for the oxygen flow dependence of NiO samples co-sputtered under similar deposition conditions.

The resistivity of the reactive co-sputtered NiFeO films and NiO decreases strongly with oxygen flow. This is similar to previous results obtained on NiO using a single deposition gun by us and others. As the decrease of the resistivity with oxygen flow is attributed to the presence of metal vacancies the results of Fig. 5 indicate that metal vacancies in NiFeO might also behave like acceptors. This suggests that the presence of the Fe atoms in the NiO matrix does not prevent metal vacancies to acts as acceptors in the NiO crystal. This hypothesis was confirmed by electric transport measurements on Au/$Ni_{0.8}Fe_{0.2}O_{1+\alpha}$/n-Si and Pt/$Ni_{0.9}Fe_{0.1}O_{1+\alpha}$/n-Si heterojunctions (see section 6) and is beyond what we expected. The large percentage of Fe in these samples (20 at%) has a significant impact on the electronic structure as shown by DFT calculations below. We are currently calculating the effect of metal vacancies on the electronic band-structure of NiFeO. More details are provided in section 8. As of the publication date of this report, the HSE-DFT calculations have not finished yet.

So, summarizing: The oxide to metal ratio of reactive RF sputtered NiFeO films is determined by the ratio of the arrival rate of oxygen and metal atoms at the substrate. The larger the pressure the larger the number of molecules and atoms that will collide with the substrate. The oxygen arrival rate at the substrate is mainly controlled by the partial pressure of oxygen in the vacuum system. The following expression provides an estimate of the number of atoms arriving at a surface area of 1 m^2 [6]:

$$\phi_{O2} = \frac{p}{\sqrt{m_{O2} kT}} \quad [1]$$

Where ϕ_{O2} is the flux of oxygen atoms incident on the surface, p is the partial O_2 pressure, m_{O2} the mass of an O_2 molecule, k the Boltzmann constant, and T the absolute temperature. The arrival rate of the metal atoms at the substrate is estimated from the deposition rate using the following expression:

$$\phi_{metal} = \frac{\rho_{metal}\, r_{QCM} \frac{\rho_{NiFeO}}{\rho_{metal}}}{m_{metal}} \quad [2]$$

Where ϕ_{metal} is the flux of metal atoms incident on the surface, r_{QCM} is the QCM deposition rate in m/sec at low oxygen flow measured with the QCM parameters set to oxide, ρ is the density kg/m^3, and m_{metal} is the mass of the metal atoms in kg/atom. Note that the factor $\rho_{NiFeO}/\rho_{metal}$ numerator converts the oxide deposition rate to a metal deposition rate

The metal arrival rate depends on the sputter yield and is also affected by the pressure in the vacuum chamber as at higher sputter pressures the beam of sputtered atoms is spread out over a larger area. Both effects are accounted for by the QCM deposition rate in equation 2. Note that this equation over-estimates the metal flux at larger oxygen flow as part of the measured QCM rate originates from the oxygen. Equation (1) under-estimates the oxygen flux as the sputtered oxygen is not included. The estimated flux-ranges for the samples sputtered at 8 mTorr and the samples sputtered at 1 mTorr are summarized in the table below. A large ϕ_{O2}/ϕ_{metal} is required to sputter samples that are fully oxidized or contain metal vacancies. NiFeO films sputtered from targets covered with an oxide layer are all highly conductive. Only for the sputter runs at high pressure and high oxygen flow rate there is a chance that the oxidation takes place in the plasma. For the other cases we would only need to consider oxidation at the substrate and/or target (see also Fig. 1 for the co-sputtering case).

Table 1: Oxygen and Metal flux at substrates for the different deposition runs. All low-pressure samples were deposited during the first half of the project. The co-sputtered high-pressure samples were deposited during the 2nd part of the project and are more homogeneous across the device wafers [6,12].

Deposition conditions	ϕ_{o2} [atom/(s m^2)]	ϕ_{metal} [atom/(s m^2)]	ϕ_{o2}/ϕ_{metal}
8 mTorr, 200 Watt, co-deposition, 0.5 sccm O_2	3.5E19	7E17	50
8 mTorr, 200 Watt, co-deposition, 20 sccm O_2	1.4E21	7E16	20,000
1 mTorr, 240 Watt, one gun, 0.5 sccm O_2	1.4E20	6E17	200
1 mTorr, 240 Watt, one gun, 2 sccm O_2	7E20	6E17	1000

4. **Optical Properties:** Optical studies have focused on three different aspects (1) transmission studies to confirm the bandgap, (2) conventional ellipsometry studies to develop a method to determine the film thickness, (3) FTIR ellipsometry studies to learn more about the oxide's phonon peaks and possibly confirm the crystal structure. The following main conclusions were drawn:

a. Transmission studies:

I. The presence of Fe in NiO is noticeable in the transmission spectra [19]. Fig. 6 below shows the effect of Fe on the transmission spectra for two high oxygen flow and for low oxygen flow sputtered samples. The jump caused by absorption across the bandgap is much sharper in the NiO spectra. This indicates that Fe doping decreases the bandgap. This statement is consistent with the results of DFT calculations performed by MSc student Fidele Twagirayezu [19, 20]. We observe a bandgap change of approximately 1.4 eV. It is easier to determine the shift from the low oxygen flow samples as oxygen vacancies appear to have a smaller effect on the transmission spectra around the bandgap than metal vacancies. This bandgap change is in agreement with the result of DFT calculations (see section 8).

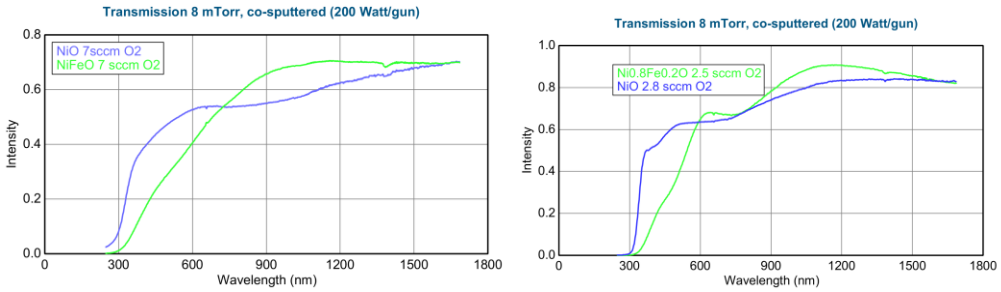

Fig. 6: Effect of Fe doping on the optical transmission of NiO for samples co-sputtered at high oxygen flow (left) and low oxygen flow (right).

II. The presence of metal vacancies is noticeable in the transmission spectra of NiFeO films by a significant change of the transmission spectrum above and below the bandgap edge [19]. For films with a significant amount of metal vacancies, the transmission increases (decreases) at shorter (longer) wavelength. See Fig. 7 below which shows the transmission spectra as a function of the wavelength for NiO and $Ni_{0.8}Fe_{0.2}O$ RF co-sputtered samples at 8 mTorr/200 Watt for different oxygen flow rates. NiFeO films sputtered above 5 sccm are believed to have metal vacancies in them. Note that these results are in agreement with recent DFT calculations on NiFeO films containing metal vacancies (see section 8 in particularly Fig. 24).

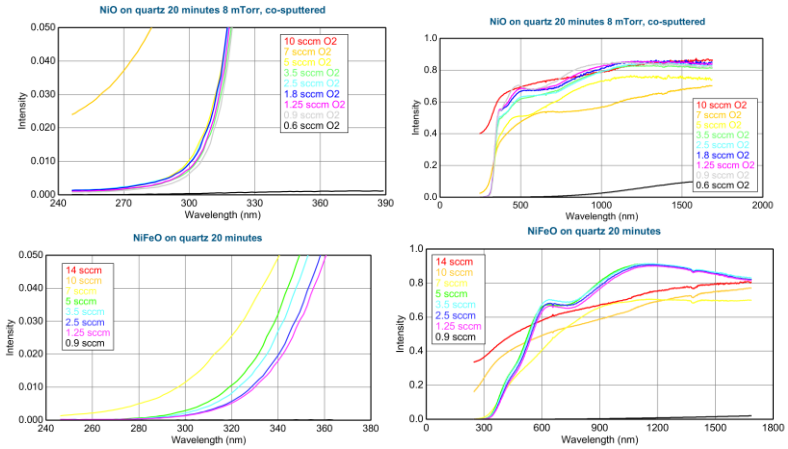

Fig. 7: transmission spectra of NiO and $Ni_{0.8}Fe_{0.2}O$ RF co-sputtered at 8 mTorr/200 Watt.

III. The presence of oxide vacancies has shown to have an effect on the optical properties of NiO by Gosch et al [21]. A new peak shows up around 2 eV for single crystalline bulk samples that are partly reduced by the annealing in vacuum at temperatures of 600 Celsius. As our samples are transparent thin film samples around 2 eV, analysis of the spectra below the band-gap edge is challenging as the calculated spectra include interference artifacts. Graduate student Yubo Cui used ellipsometry and transmission data to analyze the optical properties of RF sputtered samples and showed that a small peak between 2-3 eV might exists which depends on the oxygen vacancy concentration in the film. A peak near 2 eV is consistent with the result of DFT calculations [20,22]. Note that the data of Fig. 7 shows that the transmission is slightly lower for samples with higher oxygen vacancy concentration. This decrease in transmission stretches out over a large wavelength range from the UV to the NIR and a distinct peak is not observed. As the material is transparent in this wavelength range, peaks in the measured spectra are mainly due to interference effects in the thin film and it is difficult to separate absorption, reflection, and interference effects. We compared the measured transmission spectrum of the NiFeO film sputtered at 0.9 sccm with the calculated transmission spectra of a film with the same thickness on the same type of substrate calculated using the DFT optical properties of $Ni_{0.75}Fe_{0.25}O$ with 6.25% oxygen vacancies of Fig. 24. The calculated spectrum shows much less transmission from 300-900 nm (See Fig. 7b below) which indicates that the percentage of oxygen vacancies in our NiFeO films is significantly lower than 6.25%. From the difference in optical properties between pristine NiFeO and NiFeO with 6.25% oxygen vacancies, we estimate the oxygen vacancy concentration in these films to be well below 0.5% so much lower than anything we measured with EDAX, RBS and XPS.

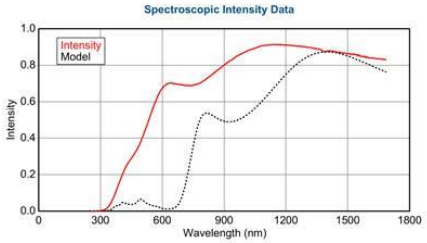

Fig 7b. Transmission spectra of 265 nm NiFeO film on glass: Measured (red) spectra on $Ni_{0.8}Fe_{0.2}O$ sample co-sputtered at 8mTorr/200 Watt with 0.9 sccm O_2 flow and calculated (DFT) spectrum of $Ni_{0.75}Fe_{0.25}O$ film with 6.25 % oxygen vacancies.

b. Conventional Ellipsometry for film thickness determination: All through the project ellipsometry was used to verify the film thickness of the samples. The following procedure appears to work well to determine the film thickness with ellipsometry: Substrate was modelled using optical files available from the Woollam materials library. The optical properties of NiO available from the literature [21] are used as initial conditions of the NiFeO layer. The NiFeO is modelled with a b-spline model with a resolution of 0.15 eV. For a first calculation the optical properties are fixed, and the film thickness is determined for which the MSE is minimum (N, C, S fit weight, force E2 positive). Then another fit is done fitting both the optical properties and the film thickness. Results converge best for films on Si/SiO_2(2 nm). For measurements on films sputtered on glass or quartz substrates, a scotch tape attached to the back during the measurements will allow us to ignore the bottom reflection when analyzing the measurement data. The thickness determined with the ellipsometer correlates well with the thickness determined by XRR (see Fig. 8a below) for thicker films. The difference between both methods is less than 5% for films thicker than 25 nm (see fig. 8 below). The thickness determined by ellipsometry also correlates strongly with the QCM thickness although it shows a large systematic error of 25%. We believe that this is caused by the fact that the QCM measures the rate approximately an inch below the exact substrate position [6,19].

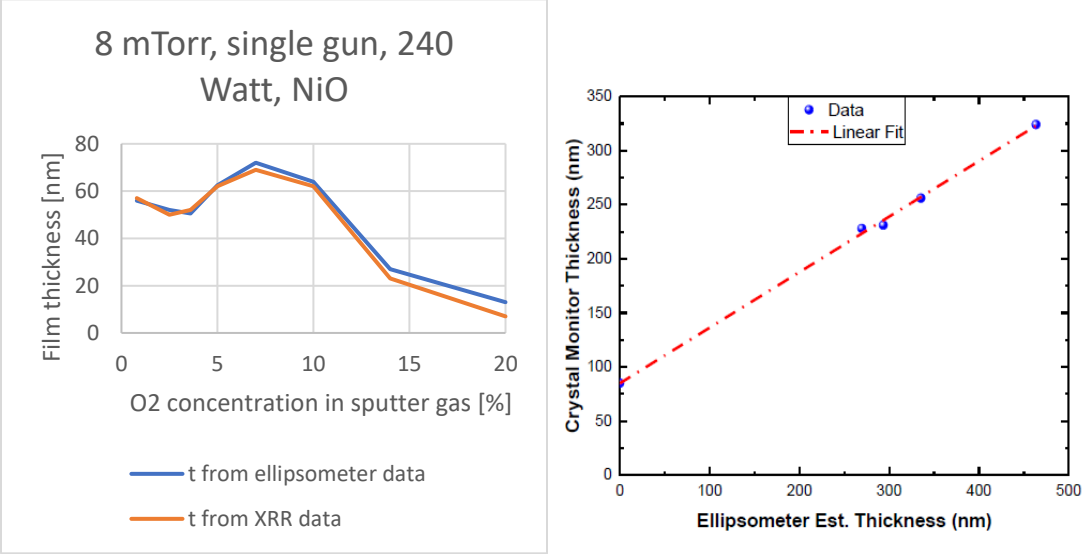

Fig. 8: (a) left: Correlation between ellipsometry and XRR thickness data [6]; (b) right: Correlation between ellipsometry and QCM thickness [19].

c. FTIR Ellipsometry study: The optical properties of NiFeO in the far-infrared were studied with an FTIR based ellipsometer. Fig. 9 below shows the measured spectra and the simulated spectra assuming a single phonon peaks in the far infrared (dashed curve). The solid curves assume no dispersion in the far infrared. The absence of the phonon peaks for Fe_3O_4 and the various phases of Fe_2O_3 is strong evidence that Fe is incorporated in the rocksalt NiO crystal structure [23] and that other phases are not present (see also discussion in section 1).

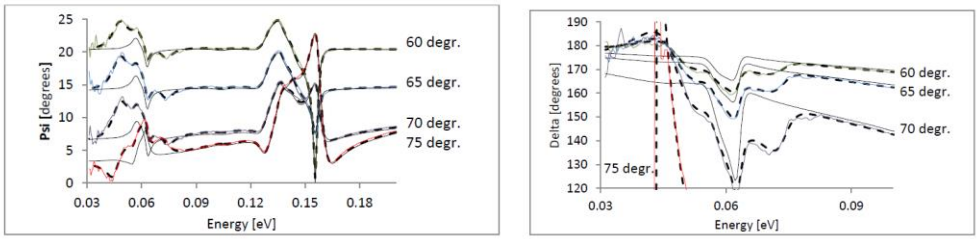

Fig. 9: Delta (left) and Psi (right) as a function of the photon energy and fits assuming a single peak phonon [23].

5. **Magnetic Properties:** The magnetic properties of RF sputtered NiO and NiFeO has been studied using two different methods, i.e. Vibrating Sample Magnetometry (VSM), and Kerr Magnetometry. The first two entries describe the main results on the as sputtered samples. The last entry relates to the effect of annealing NiFeO samples under normal atmospheric pressure.

a. Vibrating Sample Magnetometry: A method employing substrate tiles around the sample was used to suppress the magnetic signal originating from the diamagnetic silicon substrate [8]. The magnetic moment per unit volume of NiO ($Ni_{0.8}Fe_{0.2}O$) was estimated from extrapolating the high field slope to zero and estimated to be smaller than 0.5 (1) emu/cm^3 at room temperature. For NiO (NiFeO) sputtered at high oxygen flow the magnetic moment per unit volume increases with lower temperatures and is 2 (2) emu/cm^3 at 10 K. Its value depends slightly on the oxygen concentration in the films. These numbers are close to what others measured on NiFeO powders and nanoparticles [24,25]. As we see a significant difference with oxygen concentration it is believed that in particularly metal vacancies add up to the magnetic moment per unit volume in the transition metal oxides and can explain the magnetic moment of non-doped NiO particles. Fig. 10 below summarizes the magnetic moment per unit volume [8]. To the best of our knowledge, this is the first record of the magnetic properties of Fe doped NiO RF sputtered films. These results further confirm that our RF sputtered samples do not contain $NiFe_2O_4$ crystallites with a ferro-magnetic signature and are indeed anti-ferromagnetic rocksalt NiFeO. All VSM measurements were done on samples prepared with a single gun at 8 mTorr/240 Watt. Measurements were done Quantum Design PPMS system with a VSM insert on 3.5x3.5 mm^2 samples but from larger samples. All edges of the sample were sanded to remove magnetic material from them.

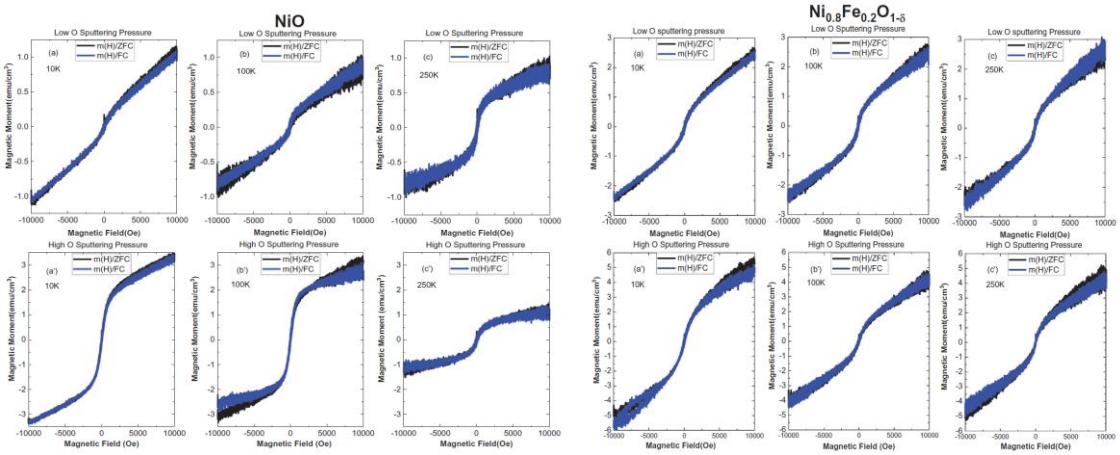

Fig. 10: Magnetic moment per unit volume of RF sputtered NiO and NiFeO thin films [8].

b. Kerr Magnetometry: A dual beam Kerr magnetometer employing a dual axis photo-elastic modulator (PEM) was designed and constructed. A Wollaston prism was used to split the beam coming from the sample is two orthogonal high-quality linearly polarized beams. A 2nd photodetector is used to measure the intensity of the 2nd beam. Theoretical calculations using Jones matrices show that the difference between the 2ω signals, is linearly proportional to Kerr rotation. This dual beam setup (see Fig. 11 below) is less susceptible to laser intensity, laser beam direction, and laser wavelength drifts [26, 27, 28].

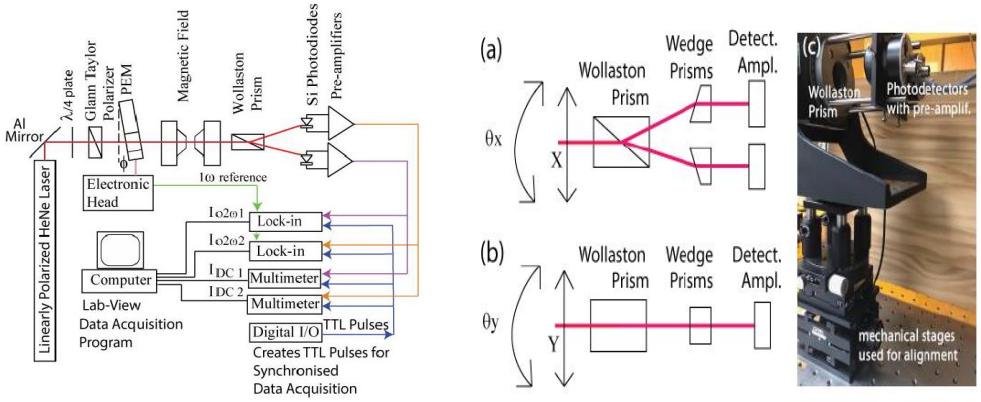

Fig. 11: Dual Beam MOKE system (left) and Analyzer-Detector system (right) [26,35].

The setup was used to measure the Faraday rotation hysteresis curve of NiFeO and NiO samples sputtered on glass microscope slides and fused quartz 1“2 coupons in fields up to 4000 Oe. The Faraday rotation of just the substrates was measured separately and subtracted from the measurement signal of the sample. The Faraday rotation of all samples was linear proportional to the field and did not show the s-curves as measured by VSM (see Fig. 10). The slope is larger for NiFeO films than for NiO films and also seems to vary with oxygen content. The linear Faraday rotation versus field observed on our samples is consistent with the results of others [29]. It is currently not clear why the Faraday rotation is not proportional to the magnetic moment of the sample. Assuming that the samples are not stoichiometric, it can be assumed that all samples have at least two types of defects. For the high oxygen flow samples, Fe substitutional dopants and metal vacancies are the dominant defect species. For the low oxygen flow samples Fe substitutional dopants and oxygen vacancies are the dominant defect species. It could be that the defects responsible for the low field s-curves measured by VSM has a negligible Faraday rotation which is overshadowed by the Faraday effect of the other type of defects. The presence of two types of defects is supported by the VSM curves which show a low field s-curve and a high field slope (see Fig. 10).

c. Effect of annealing on magnetic properties NiFeO: The phase diagram of NiFeO at atmospheric pressure shows that the NiFeO rocksalt structure is not stable beyond 2% Fe content. As the RF sputtered films reported on in this project have a much larger Fe content than this 2%, these samples are meta-stable. Note that at least one of the two states of any RRAM device is meta-stable, so this should not limit the $Ni_{0.8}Fe_{0.2}O$ from being successfully applied in devices. To investigate the effect of annealing at atmospheric pressure we measured the magnetic properties

before and after annealing the sample at atmospheric pressure with the VSM and the Kerr magnetometer system. The measurement results show that the sample becomes magnetic when annealed in the atmosphere above 500 ^{o}C (see Fig. 12 below). All measurements were done at room temperature. Preliminary results show that a magnetic anisotropy can be developed in the material when the annealing is done in a magnetic field.

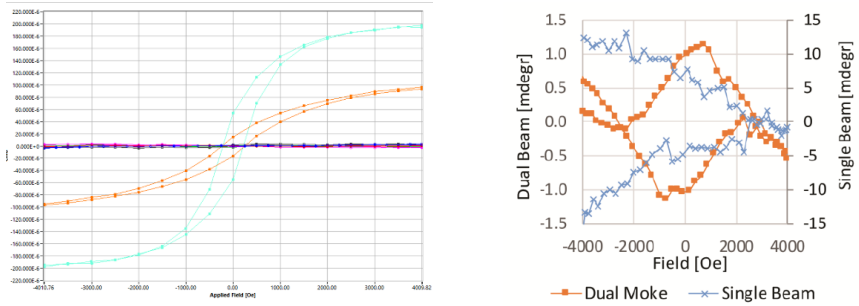

Fig. 12: Effect of annealing on Magnetic hysteresis curve of RF-sputtered $Ni_{0.8}Fe_{0.2}O$ film (8 mTorr, co-sputtered, 200 Watt/gun) (a) RT Magnetic hysteresis curve measured by VSM on sample sputtered using 2% O_2 in sputter gas after annealing at 600 ^{o}C (orange curve) and 700^{o}C (green curve) for 15 minutes in 99% Ar at atmospheric pressure (note that there is no significant magnetic fingerprint when annealing at 500 ^{o}C or lower indicating that RF sputtered NiFeO is quite stable) (b) RT Faraday hysteresis curve measured on sample sputtered using 10 % O_2 in sputter gas after annealing to 700 ^{o}C in air for 15 minutes (orange curve). Note that the curve includes Faraday background of Quartz substrate. The blue curve is the signal measured using a conventional single beam setup and in this case shows significant drift [26].

6. **Electrical Properties:** The results of linear 4-pp are discussed above in the stoichiometry-section. Here we report on IV and CV measurements done on device wafers. Preparation of those wafers was done using the following procedure: Prior to deposition the glass and quartz were cleaned with deionized water followed by a solvent clean. The 3" Silicon substrates were HF cleaned on both sides using an EDC 650 Series Spin Processor with 60 second exposure to 50:1 HF solution. Substrates were loaded in the sputtering system within two minutes of the HF clean, so no native oxygen film was present. Device wafers contained up to three different top films (i.e. $Metal_1$/Oxide/$Metal_2$). Only the top contact layer was patterned using a sheet metal deposition mask containing 32 die's each with 41 circular devices varying in radius from 400 µm to 35 µm. To promote good contact with the chuck an aluminum film was deposited on the back of some of the wafers. The oxide was co-sputtered at 8 mTorr/200 Watt. The oxygen flow during deposition was 5 sccm (low oxygen flow wafers) and 20 sccm (high oxygen flow wafers). During the deposition of the $metal_1$ and the oxide layers, microscope slides and 1x1" quartz coupons were used as shadow masks. This process resulted in the presence of silicon-NiFeO-$metal_2$, Silicon-$metal_2$, and metal1-NiFeO-$metal_2$ devices on the same wafer. For $metal_1$ and $metal_2$ Au or Pt was used. Electrical characterization was performed with a Cascade Summit 12000 probe station and Keysight B1500A Semiconductor Device Analyzer. This fully automated probe-system has instant access to each of the wafer's 1212 devices and allows for the reproducible automatic landing of the probes on the Au or Pt electrodes [16,18].

SEM pictures of the oxide do not show any pinholes and display columnar morphology with a grain size of 7-15 nm and confirm that all oxide layers are continuous (Fig. 13a). AFM measurements performed on NiFeO films sputtered under similar conditions show a roughness slightly higher than the roughness of the substrate but below 0.2 nm for films sputtered on Si and also confirm that no pin-holes are present in the NiO or NiFeO films (Fig. 13b and c).

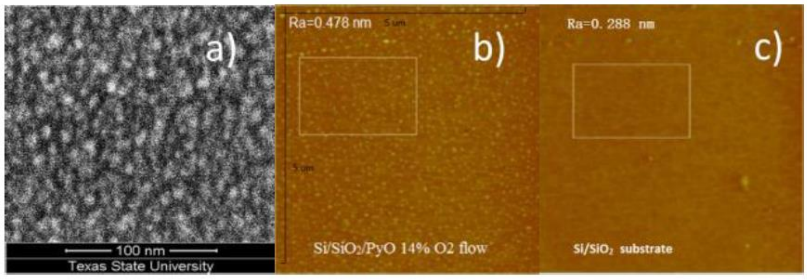

Fig. 13: (a) SEM picture of 22.4 nm thick NiFeO film sputtered at 20sccm oxygen flow (8 mTorr, co-sputtered, 200 Watt each); (b) AFM scan of Si/SiO_2/NiFeO film sputtered at 10 sccm (single gun 240 Watt); (c) AFM scan of Si/SiO_2 bare substrate [6,8].

a. <u>IV measurements:</u> Typical IV-curves for Si-NiFeO-Au devices are shown in Fig. 14 below. Strong rectification is observed on devices on n-type Si while devices on p-Si show as small rectification. Both devices on n-Si and p-Si using low oxygen flow NiFeO show significant hysteresis in the IV-curve.

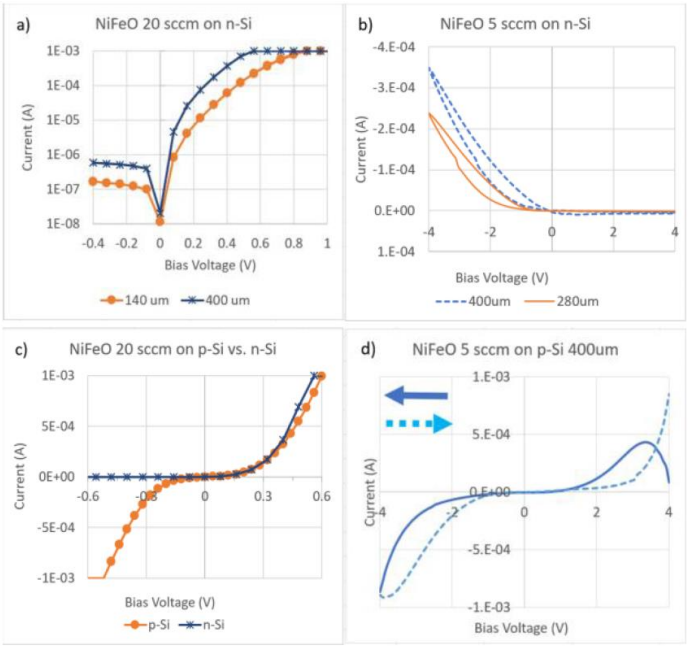

Fig. 14: IV curves of Si-NiFeO-Au devices: (a) n-$Si/Ni_{0.8}Fe_{0.2}O_{1+\alpha}$; (b) n-$Si/Ni_{0.8}Fe_{0.2}O_{1-\alpha}$; (c) p-$Si/Ni_{0.8}Fe_{0.2}O_{1+\alpha}$; (d) p-$Si/Ni_{0.8}Fe_{0.2}O_{1-\alpha}$ [16,18].

The IV curves for n-Si/$Ni_{0.9}Fe_{0.1}O_{1+\alpha}$/Pt are very similar to the n-Si/$Ni_{0.8}Fe_{0.2}O_{1+\alpha}$/Au devices although both have a different work-functions (ϕ_{Au}=4.5 eV and ϕ_{Pt}=5.6 eV). In order to determine whether the n-Si/NiFeO or NiFeO/metal interface is responsible for the rectifying properties the IV curve of Pt/$Ni_{0.9}Fe_{0.1}O_{1+\alpha}$/Pt devices were measured and a typical curve is shown in Figure 15 below. Note that the metal/semiconductor contact is completely Ohmic for voltages below 0.02 Volts. The relatively large current densities indicate that no Shottky barrier exists for $Ni_{0.9}Fe_{0.1}O_{1+\alpha}$/Pt. Assuming the case is similar for $Ni_{0.8}Fe_{0.2}O_{1+\alpha}$/Au it can be concluded that the rectifying properties of Fig. 14a originate from the n-Si/NiFeO heterojunction.
The small rectifying properties of devices on p-type silicon suggest that $Ni_{0.8}Fe_{0.2}O_{1+\alpha}$ is p-type and a negligible barrier exists for the flow of holes. From recent work on Si/NiO heterojunctions [30] it is known that the valence band edges of Si and NiO line up with each other. The here presented results indicate that also the valence band edges of Si and NiFeO line up with each other. The strong rectifying effect of the n-Si/$Ni_{0.8}Fe_{0.2}O_{1+\alpha}$ heterojunction indicates that the conduction band edge of both materials are not lined up with each other and the conduction band contains a significant one-way barrier for charge transport.

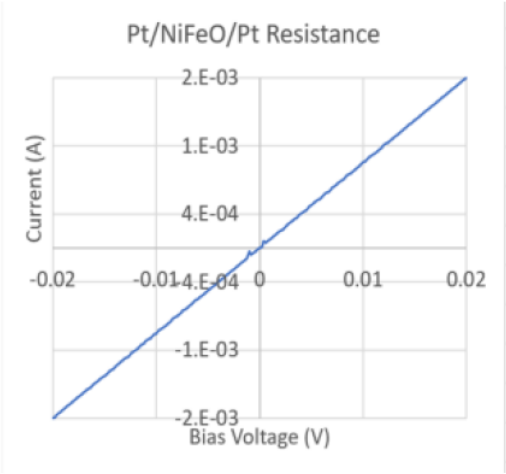

Fig. 15. IV curve of Pt/$Ni_{0.9}Fe_{0.1}O_{1+\alpha}$/Pt device [16]

The measurement result of Fig. 15 include the bulk resistance of the NiFeO ($\frac{\rho_{NiFeO}t}{A}$), the contact resistance between the metal electrodes and the NiFeO ($2\frac{r_{NiFeO-Pt}}{A}$), and the contact resistance of the probes with the top electrodes ($2R_{probe}$). The total two-point-probe resistance is given by:

$$R_{2pp} = \frac{\rho_{NiFeO}}{A} + 2\frac{r_{NiFeO-Pt}}{A} + 2R_{probe} \approx \frac{\rho_{NiFeO}}{A} + 2\frac{r_{NiFeO-Pt}}{A} \quad [3]$$

Reorganizing equation [3] and using the resistivity from the linear 4pp measurements on NiFeO films on quartz gives an expression for the specific contact resistivity for the NiFeO-metal contacts:

$$r_{NiFeO-Pt} = \frac{A(R_{2pp}-2R_{probe})-\rho_{NiFeO}t}{2} = \frac{A(R_{2pp}-2R_{probe})-\rho_{4pp}t}{2} \quad [4]$$

Using the data of Fig. 15 and the data for linear 4pp measurements for the resistivity we found for the specific contact resistivity of $Ni_{0.9}Fe_{0.2}O_{1+\alpha}$/Pt contact 0.0007+/-0.0003 Ω cm^2. To our knowledge, this is the first reported contact resistivity to NiO or doped NiO films.

Although the IV curves shown in Fig. 14a and b look like exponential diode curves, Semi-log plots show that they are not exponential. Log-Log curve show that they better obey a power law and that the IV characteristic is almost proportional to V^2 with a linear IV relation for very small voltages (see Fig. 16 below). The critical voltage beyond which Ohm's behavior is replaced by a voltage square law was used to estimate the mobility using the method detailed in [31]. A value of 9E-4 cm^2/Vs was estimated for the mobility of the RF sputtered NiFeO [18]. Note that this method assumes all injected charges are mobile which is not the case if a significant number of shallow traps are present. So, we expect the actual mobility to be larger than this value.

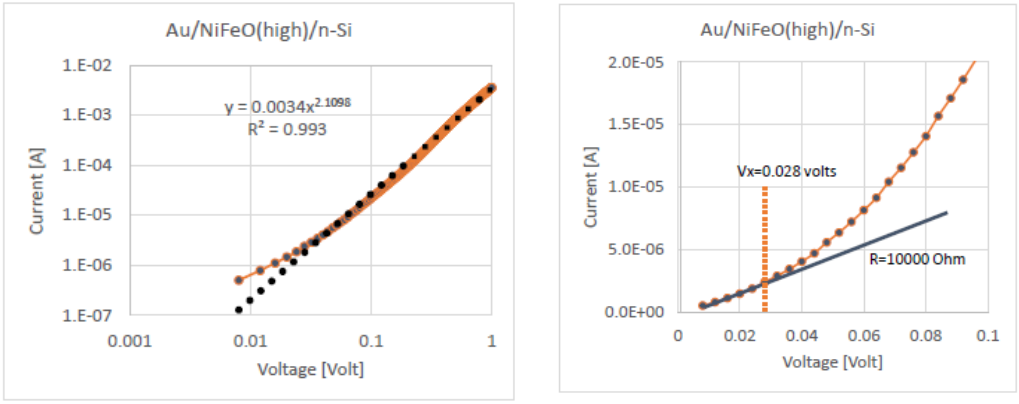

Fig. 16: IV curve of n-Si/$Ni_{0.8}Fe_{0.2}O_{1+\alpha}$ [18].

For devices sputtered at low oxygen concentration, the ascending curves in the IV plot are largely exponential while the descending curves better follow a power fit.

b. CV measurements: The CV data was used to determine built-in voltage and the carrier concentration of the NiFeO using an analysis based on heterojuctions as described in [31]. The average built-in voltage of n-Si/$Ni_{0.8}Fe_{0.2}O_{1+\alpha}$/Au devices was approximately 0.76 Volt and 0.13 volt higher than the built-in voltage of n-Si/Au devices. The slope of the CV curves for both types of devices was similar which could be a coincident as we expect the carrier concentration in the p-NiFeO to be similar to that in the n-Si. The estimated hole and electron concentrations in NiFeO and Si using various models are summarized in Figure 17 below. Using the hole concentration of Fig. 17 and the resistivity from linear 4pp measurements, the estimated hole mobility is 8E-3 cm^2/Vs [18], so a factor 10 higher than the mobility determined from transition voltage observed in the IV curve. The small difference in slope in the CV graph between devices with and without NiFeO suggests that maybe no significant depletion area exists in the NiFeO and CV curves only tell us the carrier concentration of the silicon. So, a more thorough CV study on devices sputtered at different oxygen flow concentration and devices produced with NiO is desirable and required before this part of the work is publishable.

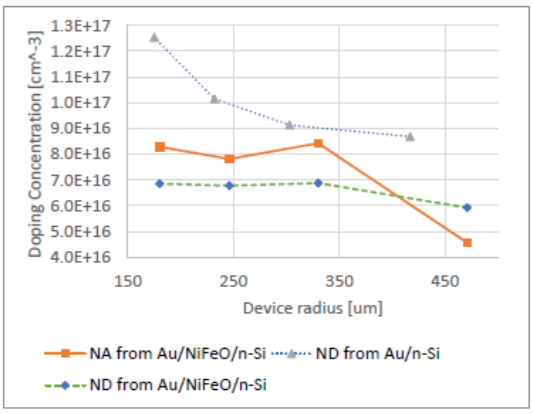

Fig. 17: Carrier concentration of n-Si/$Ni_{0.8}Fe_{0.2}O_{1+\alpha}$ sputtered at 8 mTorr, two guns, 200 Watt each, and 20 sccm oxygen flow [18].

c. Implications of electrical properties for applications:

1. The rectifying properties of n-Si/NiFeO junctions might be useful for selection purposes in RRAM devices. Further useful applications of the rectifying effects are as an electron blocker in solar cells and photodetectors similar to the recent proposed use of n-Si/NiO heterojunctions [30].
2. Although up to no systematic study was performed after the resistance switching properties of our films under large voltage sweeps, switching between a high and low resistance state was observed in low oxygen flow samples on n-Si in quasi-static voltage scans. We believe that this switching is of the type 1 RS mechanism where oxygen vacancies modulate the barrier height and width in the device [32,33,34].

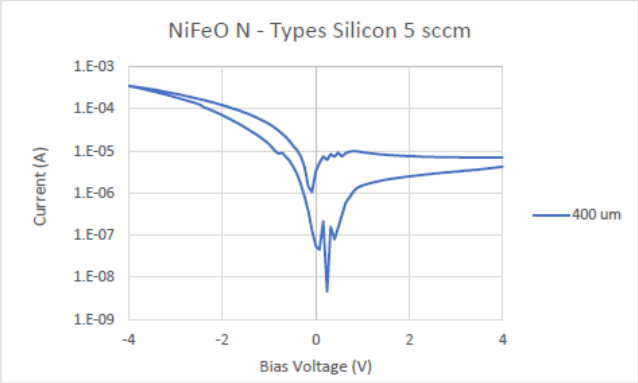

Fig. 18: Resistive switching and diode behavior in log(I) vs V plot for a n-Si/$Ni_{0.8}Fe_{0.2}O_{1-\alpha}$ device [18].

7. **Electronic band structure calculations by DFT on the NiO and Fe-doped NiO system:** In support of the experiments the electronic structure was calculated for NiO without and with oxygen vacancies, Fe doped NiO, NiFeO with oxygen vacancies, NiO with metal vacancies, NiFeO with metal vacancies, NiO with O or Ni interstitials, and NiO with charged oxygen vacancies. All calculations are done within Density Function Theory (DFT) using the Vienna Ab initio

Simulation Package (VASP) and the Projector Augmented Wave (PAW) method in conjunction the Generalized Gradient Approximation (GGA) of Perdew, Berke and Ernzerhoff (PBE) for exchange and correlation [37,38,39,40]. Additional calculations were performed using the HSE06 method. The results GGA+U calculations are summarized below for the various calculations.

a. Effect of Oxygen vacancies in NiO: Oxygen vacancies introduce occupied states in the bandgap just below the Fermi level effectively decreasing the bandgap from 3.29 to 1.84 eV. The impact on the optical properties is shown in Fig. 19c below and includes a slight red shift of the main absorption peak (0.25 eV) and the introduction of a new peak near 1.85 eV. These results are consistent with the experimental results of Gosh on the optical properties measured on a single crystalline NiO bulk sample [21].

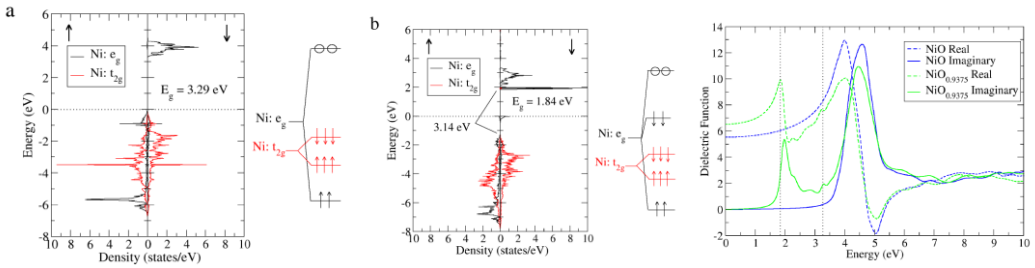

Fig. 19: Electronic structure of pristine NiO (a), $NiO_{0.9375}$ (b), Calculated optical spectra (c) [20,40,17].

b. Effect of Fe substitutions in NiO: Substitutional Fe dopant creates states in the bandgap of NiO just below the Fermi-level effectively reducing the bandgap of the oxide to 2.26 eV. The bandgap is effectively decreased to 2.26 eV. Note that these results correlate very nicely to the experimental transmission data shown in Fig. 6 [17, 20].

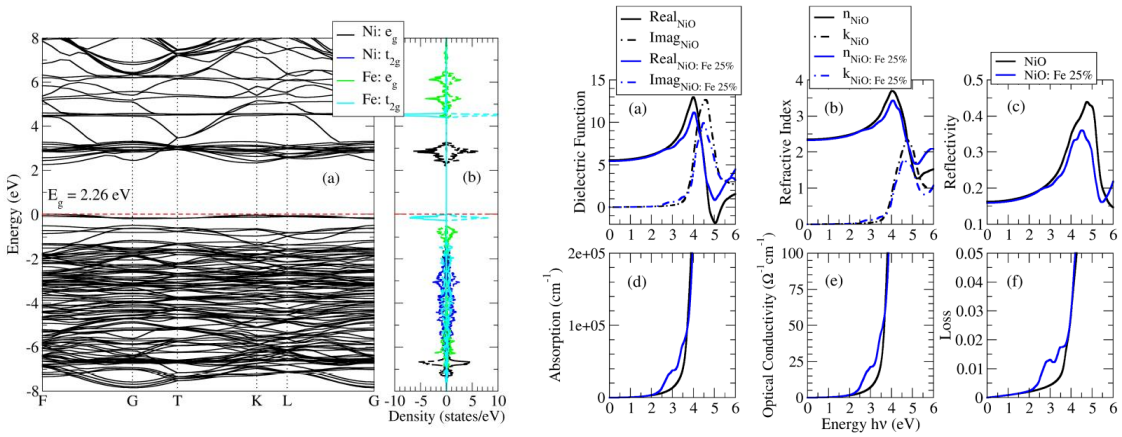

Fig. 20: Effect of Fe doping (25%) on the electronic bandstructure of NiO (a) and the effect on the optical properties (b) [20].

c. Effect of oxygen vacancies in NiFeO: The effect of oxygen vacancies in NiFeO is similar to NiO and reduces the effective bandgap. Occupied states a little above the valence band of pristine NiFeO and empty states a little below the conduction band edge of pristine NiFeO. No redshift

was observed in the optical spectrum for the main peak. Similar to NiO, optical vacancies however, create a peak around 2 eV in the optical spectrum (see Fig. 21 below) [17, 40].

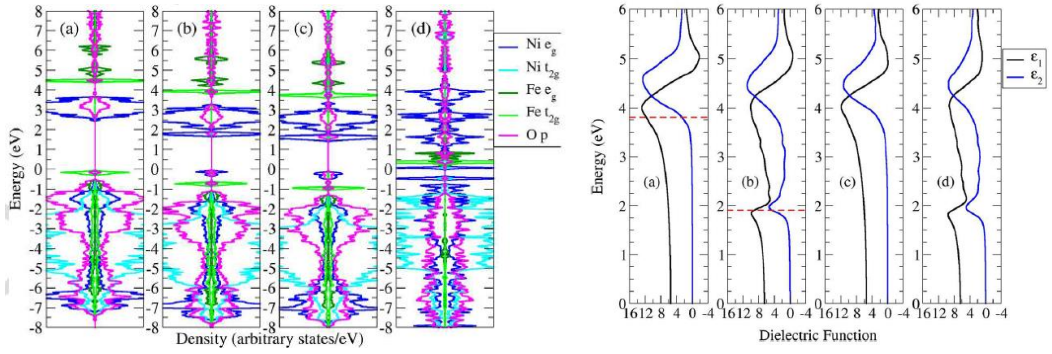

Fig. 21: Effect of oxygen vacancies (0%, 6.25%, 12.5%, and 25% V_O) on the electronics bandstructure (left) and effect of oxygen vacancies on optical properties of NiO (0%, 6.25% V_O) and NiFeO (0%, 6.25% V_O) (right) [40].

A charge density plots for this material is shown in Fig. 22 below using a 4 A slice along the (-111) plane. The states caused by the oxygen vacancy are not only found at a discrete location, but do not perturb the surrounding charge distribution. Thus, these states are localized with the Fe-doped system as with the pristine material [41]. This behavior is also confirmed here by looking at the charge density plots for the state corresponding to the valence band maximum and conduction band minimum, with both showing a similar degree of localization around the defect. It is expected that either of those states are deep traps and either act as charging or discharging centers our biased heterojunction devices [22]. Note that the existence of traps in NiFeO films with oxygen vacancies is in agreement with the observed hysteresis in the IV-curves of Si/$Ni_{0.8}Fe_{0.2}O_{1+\alpha}$ heterojunctions prepared at low oxygen flow as reported on in section 6.

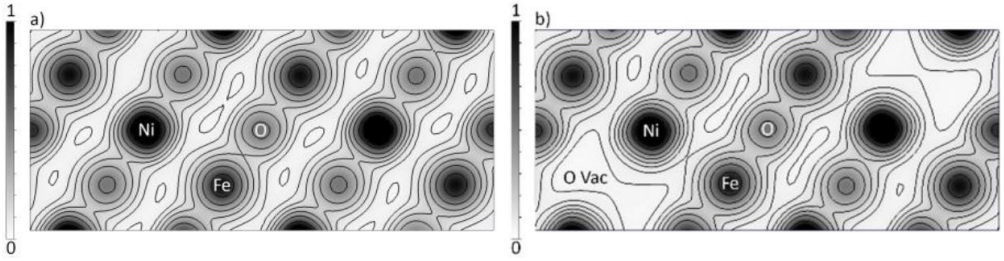

Fig. 22: Total Charge densities in $Ni_{0.81}Fe_{0.19}O$ (a) without oxygen vacancies and (b) with Oxygen vacancies. Ni atoms correspond to darker regions, Fe atoms correspond to less dark regions and O atoms correspond to the lightest of the three circular regions [22].

d. <u>Effect of metal vacancies in NiO:</u> In NiO, metal vacancies create unoccupied states slightly above the valence band edge and slightly below the conduction band edge. Because of the latter the bandgap is slightly reduced. The empty states above the valence band edge act like acceptors and are responsible for the p-type electric properties of NiO films prepared under high oxygen flow conditions. Fig. 23 below shows the calculated electronic structure for pristine NiO and NiO

with metal vacancies on the left and middle, and the calculated absorption spectra on the right. Note that the metal vacancies reduce the absorption in the UV and increase the absorption in the visible part of the spectra.

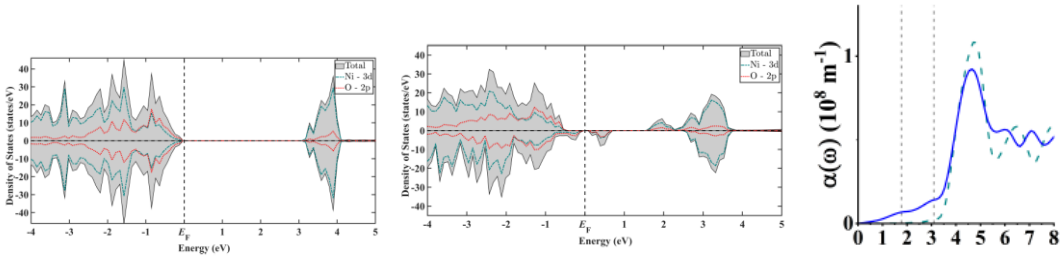

Fig. 23: Electronic bandstructure of pristine NiO (left), electronic bandstructure of NiO with Ni vacancies (middle) and calculated optical properties of pristine (dashed) and NiO with Ni vacancies (blue) (right) [22,17].

e. <u>Effect of metal vacancies in NiFeO:</u> DFT calculations show that metal vacancies in NiFeO create occupied states above the original valence band edge of NiFeO and unoccupied states below the conduction band edge. Note that the states above the valence band edge are occupied and thus do not act as acceptors as is the case in NiO. The results are summarized in Fig. 24 below. These results suggest that metal vacancies do not act as acceptors, in contradiction to the experimental results. The HSE06 calculation on the similar system is still running. It could be that Fe shifts the acceptors level down similar to other dopants in NiO such as Cu [42]. As Fig. 24 are the results of a DFT calculation using GGA+U, the calculated shift might be an overestimate, so we are currently performing a HSE60 calculation on the same system. Note that our experimental results show that NiFeO sputtered at high oxygen flow is highly conductive (see Fig. 5). Also, the IV properties of n-Si/$Ni_{0.8}Fe_{0.2}O_{1+\alpha}$/Au devices suggest that NiFeO sputtered at high oxygen flow is p-type.

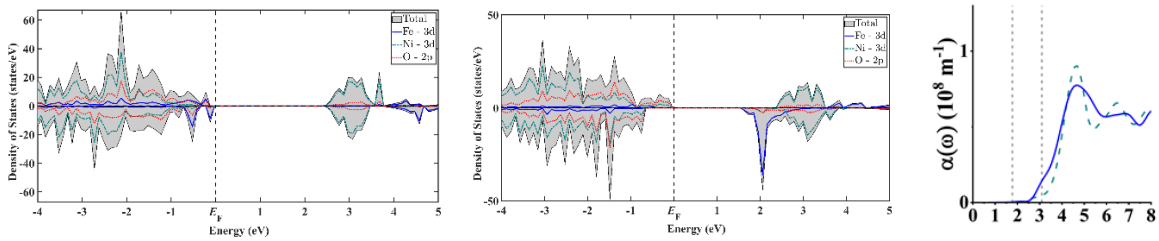

Fig. 24: Electronic bandstructure of pristine $Ni_{81.25}Fe_{18.75}O$ (left), electronic bandstructure of NiFeO with metal vacancies (middle) and calculated optical properties of pristine NiFeO (dashed) and $Ni_{75}Fe_{18.75}O_{100}$ (includes 6.25% Ni vacancies compared to (a)) (blue) (right) [22].

f. <u>Effect of Ni-interstitials in NiO:</u> DFT calculations show that Ni interstitials in NiO create empty states just below the conduction band edge of NiO and occupied state just above the valence band edge of NiO effectively decreasing the bandgap to 1.1 eV. The bandstructure is similar to

that of NiO with metal vacancies but the Fermi-level is in the bandgap so no p-type behavior for NiO with Ni interstitials. The results are summarized in Fig. 25 below.

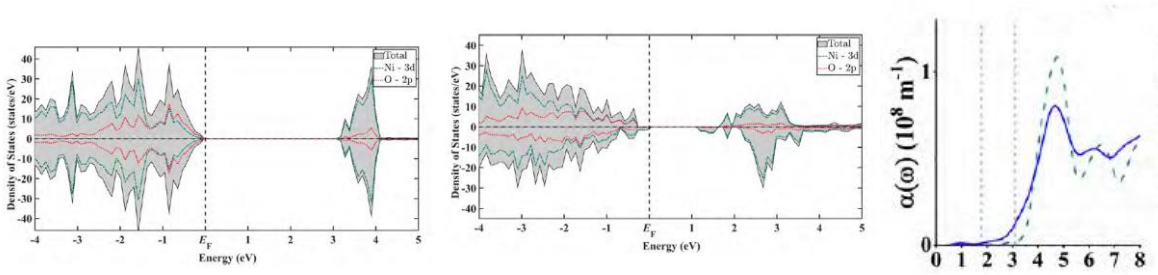

Fig. 25: Electronic bandstructure of pristine NiO, NiO with Ni interstitials and optical properties of pristine NiO (dashed) and $Ni_{106.25}O_{100}$ (with Ni interstitials) (blue) [22].

g. <u>Effect of O-interstitials:</u> O interstitials have less of an effect on the bandgap and the optical properties as most changes happen below or above the original bandgap of pristine NiO. Results are shown in Fig. 26 below.

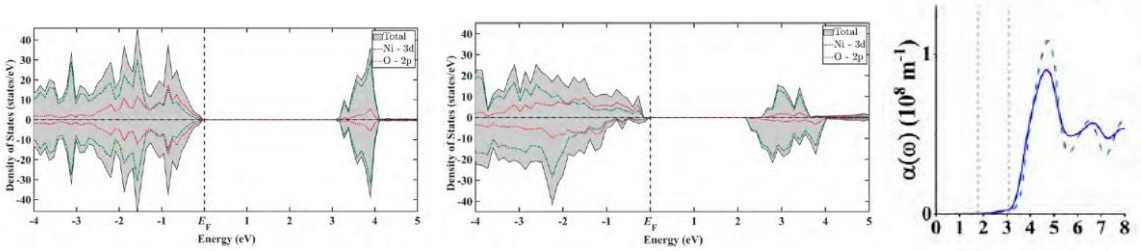

Fig. 26: Electronic bandstructure of pristine NiO and NiO with O interstitials, and optical properties of pristine NiO (dashed) and $Ni_{100}O_{106.25}$ (with O interstitials) (blue) [22].

h. <u>Effect of charged oxygen vacancies:</u> Charged oxygen vacancies (O^{2+}) introduce unoccupied states in the middle of the bandgap. Note that there is very little difference between the bandstructure of the NiO with oxygen vacancies and with charged oxygen vacancies (see Fig. 27). The optical properties vary with the charge state (see fig. 28). It would be interesting to see if we can measure those effects experimentally. For this we would need to deposit the NiFeO on a transparent conductor such as for example ITO. Optical measurements should be taken with and without electrical bias to the thin film sandwich.

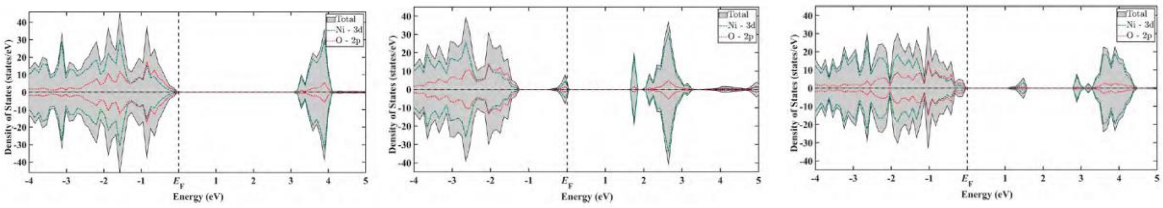

Fig. 27: Bandstructure of pristine NiO, $Ni_{100}O_{93.75}$ (with neutral oxygen vacancies), and $Ni_{100}O_{93.75}^{2+}$ with charged oxygen vacancies [22].

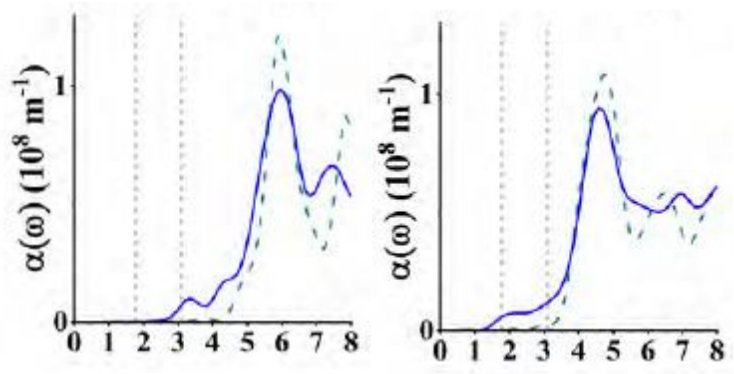

Fig. 28: Comparison of optical properties of pristine NiO (dashed curves) with the optical properties of NiO with neutral oxygen vacancies (left) and charged oxygen vacancies (O^{2+}) (right) [22].

8. **Electronic band structure calculations by DFT on other dopants in NiO:** DFT calculations were also done for Ag, Cu and C doped NiO. Both Ag and Cu substitutional dopants for Ni act like acceptors (empty states in the bandgap above the valence band edge) while C substitutional dopant replacing Ni introduces occupied states below the valence band edge. The calculated band-structures using GGA+U suggests that acceptors of Ag dopants will have the lowest ionization energy [22] while the ionization energy of the Cu acceptor is more than 1 eV. Others however have shown that Cu doping lowers the energy level of Ni-vacancies putting them closer to the valence band edge, effectively increasing the free hole concentration at room temperature. The effect of Cu and Ag doping on the optical properties is much larger than the effect of Fe doping as shown in Fig. 29 below.

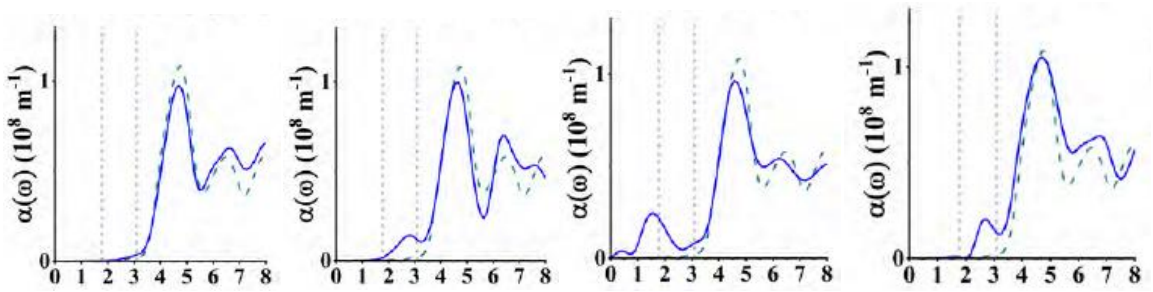

Fig. 29: Optical properties of Fe doped (12.5%), Cu doped (12.5%), Ag (12.5%), and C (6.25%) doped NiO for each graph compared to the optical properties of pristine NiO [22].

DFT calculations were also done for C atom replacing O in NiO. This substitution leads to the introduction of an empty state in the bandgap that can act like an acceptor state. Note however that C on an oxygen site is energetically much less favorable than C on a Ni-site [22].

9. **Spin-offs:** Both the computational and experimental projects lead to other projects. In particular, we recognize the following spin-offs and parallel studies that lead to other grants and/or peer reviewed publications:

a. During the course of the project, we provided project summaries for three DOD instrumentation proposals that were all awarded: (1) "Full-Spectrum Electrical Characterization Station for Device and Material Studies in Research and Education " (70479-RT-REP), DOD proposal of Dr. Jian Li; (2) “Scanning Probe Microscope for Materials Research and Education” (68869-RT-REP), ARO proposal Dr. Alex Zakhidov; (3) “Acquisition of a Fourier- Transform Infrared Ellipsometer with Cryostat for Research and Education” (68840-RT-REP), Army Research Office proposal Dr. Stefan Zollner. The project greatly benefited from (1) and (2) and we hope to use the FTIR ellipsometer at New Mexico State in the summer of 2020 for additional measurements on annealed NiFeO thin films.

b. Undergraduate students David Torres and Cole Stevenson refurbished an old VSM that facilitated the first magnetic measurements done on the NiFeO films. Their preliminary results were included in an NSF-MRI proposal for a new VSM which was awarded in 2017.

c. Graduate student James Shook calculated the electronic and optical properties using DFT of similar oxides including Cu and Ag based delafossites, $CuAlO_2$, $AgAlO_2$, $CuCrO_2$ and $AgCrO_2$. His studies were focused on investigating the role of metal and oxygen vacancies, as well as the effects of Magnesium doping. This was a parallel project with which we have learned a lot about the role played specially by O vacancies in these oxides [43, 44, 45].

d. When studying the magneto-optical properties of NiFeO thin films, graduate student Ahad Talukder successfully modeled the multiple interference effect in a photoelastic modulator [27, 28]. Using his model, graduate student Shankar Acharya and undergraduate student Brian Collier designed and constructed a dual beam Magneto-Optical Measurement setup. Such setup is less susceptible to light source drift, including laser intensity, laser wavelength, and laser pointing stability drifts caused by temperature variations in the lab [26].

e. When studying the magnetic properties of NiFeO thin films, graduate student Binod D.C. and High School student Sarah-Beth Ragan developed a model to describe the effect of sample/sample-rod wobble on the torque magnetometer measurements performed with a biaxial vibrating sample magnetometer. This model let to an invention disclosure with the university for a new method to determine sample position in a biaxial VSM [46].

10. Suggestions for further research:

a. Further research on transition metal oxides should (1) focus on further optimizing the metal atom flux across the substrate possibly by installing a 4 inch sputter gun that is mounted directly below the substrate holder; (2) develop a method to determine the metal flux distribution across the substrate holder; (3) re-evaluate the oxygen inlets to facilitate a homogeneous oxygen flow on the substrate; (4) develop a method to determine the oxygen flux distribution across the substrate holder; (5) The analysis summarized in Table 1 is not very accurate and a more complete model needs to be developed to better understand how the oxygen or metal vacancy concentration of reactive RF sputtered transition metal oxides depend on deposition parameters including sputter power, sputter pressure, number of sputter guns and oxygen gas inlets.

b. Deposition of thicker films to determine the optical properties of NiFeO bulk films with oxygen or metal vacancies. The objective here is to develop this in a method to determine vacancy concentrations from optical properties. The results presented in this final report suggest that this method might be more feasible than chemical concentration analysis using Edax, RBS, or XPS. Magnetic methods to determine vacancy concentrations as we pursued early on in the project are not sensitive enough as indicated by the results in section 5 of this final progress report.

c. Characterization of magnetic anisotropy and electric transport properties of NiFeO thin films that are annealed in a magnetic field. Such a system will be inhomogeneous and might have interesting magnetoresistance properties. It would also be interesting to explore how ion transport in these systems will affect the magnetic moment of these films and the magnetoresistance.

d. To fully understand the rectifying properties of NiFeO/n-Si heterojunctions a systematic study needs to be performed on how the oxygen flow during deposition affects the band-offset of Si and NiFeO. Note that it is well known in the literature that oxygen plasma treatments of thin films affect the work function and electron affinity, and thus the band offset in heterojunction devices. These experimental results will have to be accompanied by DFT calculations on the band-offset between NiFeO and Silicon.

e. The measured mobility although a low value estimate is very low compared to other semiconductors. It would be useful to explore if it is possible to create thin films with larger grains that have less grain boundary scattering and thus a higher mobility. Studies of depositions performed at higher temperature should be performed. Such studies should include the investigation of films that are thicker and or films that are grown epitaxially.

f. The switching properties of Pt/NiFeO/Pt RRAM devices should be further investigated. It would in particularly be interesting to focus on devices that have their oxide sputtered at lower oxygen flow rate, i.e. 2.5 sccm. The devices reported on in the current study have too much leakage current making type 1 RS the only observable switching mechanism. The results shown in Fig. 5 show that devices with a 10 times larger resistivity can be produced by decreasing oxygen flow during deposition. Such research should include (1) dynamic IV measurements. So far all our IV measurements have been performed in quasi-static mode using a semiconductor device analyzer sweeping the voltage at low speed; (2) temperature dependent IV measurements to detect the formation of metallic filaments in the RRAM devices; (3) impedance spectroscopy measurements as a function of the temperature to determine the motion of ions in the thin films; (4) DFT calculations to determine the mobility of atoms along grain boundaries. Up to now all DFT calculations on atom transport were bulk based for a system without grain boundaries.

g. The preliminary DFT results on the effect of other dopants in NiO are interesting and suggest that other dopants including Cu, Ag, and C have a much stronger effect on the optical properties than Fe. To further explore the effect of Fe doping the following activities should be explored: (1) direct confirmation by Hall and/or MR measurements that NiFeO sputtered at high oxygen flow contains holes; (2) a systematic study how the freeze out of carriers depend on the iron concentration and determination of the acceptor ionization energy from these measurement results; (3) DFT-HSE60 calculations after the effect of Fe doping on the ionization energy of metal vacancies. So far only a GGA+U calculation for $Ni_{75}Fe_{18.75}O_{100}$ was completed which did not show unoccupied acceptor states in the bandgap. The HSE60 calculation for the same system is still not completed. It would also be interesting to investigate the effect of lower metal vacancy concentrations; (4) a systematic study after how Ag and Cu doping affects the ionization energy of Ni vacancies in NiO by DFT and by experiment.

References:

[1] Maclyn Compton, Nelson Simpson, Elizabeth Leblanc, Michael A. Robinson, Wilhelmus J. Geerts, "Electrical and Optical Properties of Permalloy Oxide grown by dual ion beam sputtering", Materials Research Society Symposium Proceedings 1708 (2014), mrss 14-1708-VV08-01 (6 pages), doi:10.1557/opl.2014.621.
[2] V. Raghavan, "Fe-Ni-O (Iron-nickel-oxygen)", J. Phase Equilibria Diffus. 31 (2010) 369-371.
[3] Zhang Song, Tiphaine Bourgeteau, Itaru Faifuku, Yvan Bnnassieux, Erik Johnson, Yauaki Ishikawa, Martin Fodyna, Pera Roca I Cabarrocas, Ykiharu Uraoka, Thin Solid Films 646 (2018) 209-215.
[4] M.L. Grilli, F. Menchini, T. Dikonimos, P. Nunziant, L. Pilloni, M. Yilmaz, A Piegari, A. Mittiga, "Effect of growth parameters on the properties of RF-sputtered highly conductive and transparent p-type NiOx films, Semicon. Sci. Technol. 31 (2016) 055016 (10p).
[5] Hao0Long Chen, Yang-Ming Lu, Jun-Yi Wu, Weng-Sing Hwang, "Effects of Substrate Temperature and Oxygen Pressure on Crystallographic Oientations of Sputtered Nickel Oxide Films", Mat. Trans. 46 (2005), pp. 2530-2535.
[6] Md. Abdul Ahad Talukder, "Influence of oxygen flow on the microstructure, resistivity, and Faraday rotation of reactive RF sputtered NiO and Fe-doped NiO thin films", thesis Texas State University, San Marcos, December 2017.
[7] Binod D.C., "The Magnetic Characterization of Permalloy and Permalloy Oxide Grown by RF Magnetron Sputtering", thesis Texas State University, San Marcos, December 2019.
[8] Fidele J. Twagirayezu, Md. Abdul Ahad Talukder, Wilhelmus J. Geerts, "Magnetic Properties of RF sputtered NiO and Ni0.8Fe0.2O1-d samples grown on SiO2/Si substrates, published in Materials Research Innovations, July 19 2018, https://doi.org/10.1080/14328917.2018.155879
[9] S.C. Chen, C.K. Wen, T.Y. Kuo, W.C. Peng, H.C. Lin, "Characterization and properties of NiO films produced by rf magnetron sputtering with oxygen ion source assistance", Thin Solid Films 572 (2014) 51-55.
[10] S. C. Chen, T. Y. Kuo, Y. C. Lin, H. C. Lin, "Preparation and properties of p- type transparent conductive Cu-doped NiO films", Thin Solid Films 519 (2011), 4944-4947.
[11] Binod D.C., Andres Oliva, Anival Ayala, Shankar Acharya, Fidele Twagirayezu, James Nick Talbert, Luisa M. Scolfaro, Wilhelmus J. Geerts, "Magnetic Properties of reactive co-sputtered NiFe-oxide samples", IEEE Trans. on Magn. 55 (2019) 2900205, pp. 2900205-1-6, DOI: 10.1109/TMAG.2018.2866788.
[12] Yubo Cui, Electrical and Optical Properties of RRAM, Thesis Texas State University, San Marcos, summer 2016.
[13] P. Hovington, D. Drouin, R. Gauvin, D. C. Joy, and N. Evans, "CASINO: A new monte Carlo code in C language for electron beam interactions-part III: Stopping power at low energies," *Scanning*, vol. 19, no. 1, pp. 29–35, 2006. 169
[14] D. Drouin, A. R. Couture, D. Joly, X. Tastet, V. Aimez, and R. Gauvin, "CASINO V2.42 - A fast and easy-to-use modeling tool for scanning electron microscopy and microanalysis users," *Scanning*, vol. 29, no. 3, pp. 92–101, 2007.
[15] R. Gauvin, "What Remains to Be Done to Allow Quantitative X-Ray Microanalysis Performed with EDS to Become a True Characterization Technique?," *Microsc. Microanal.*, vol. 18, no. 05, pp. 915–940, 2012.

[16] James N. Talbert, Samuel R. Cantrell, Md. Abdul Ahad Talukder, Luisa M. Scolfaro, Wilhelmus J. Geerts, “Electrical Characterization of Silicon – Nickel Iron Oxide Heterojunctions”, MRS Advances 4 (2019) 2241-2248, DOI: 10.1557/adv.2019.321
[17] John Petersen, “Impurities in Antiferromagnetic Transition-Metal Oxides – Symmetry and Optical Transitions”, dissertation Texas State University, December 2017.
[18] Nick Talbert, “Electrical Characterization of Nickel Oxide and Nickel Iron Oxide thin films and resistive random access memory devices grown by Radio Frequency Sputtering”, thesis TxState University, San Marcos, Dec. 2019.
[19] Fidele Twagirayezu, Theoretical and Experimental Determination of Properties of NiO and Fe-doped NiO”, thesis Texas State University, San Marcos, August 2017.
[20] John E. Petersen, Fidele Twagirayezu, Luisa M. Scolfaro, Pablo D. Borges, Wilhelmus J. Geerts, “Electronics and Optical properties of antiferromagnetic Iron doped NiO – A first principles study”, AIP Advances 7, (2017) 055711-1-5; doi:http://dx.doi.org/10.1063/1.4975493.
[21] A. Ghosh, C.M. Nelson, L.S. Abdallah, and S. Zollner, “Optical constants and band structure of trigonal NiO”, J. Vac. Sci. and Techn. A 33 (2015) 0612203.
[22] Sam Cantrell, “Optoelectronic Properties and Energetics of Defects and Impurities in NiO studied using Ab Initio Calculations”, thesis Texas State University, December 2019.
[23] Md. Abdul Ahad Talukder, Yubo Cui, Maclyn Compton, Luisa Scolfaro, Stefan Zollner, Wilhelmus J. Geerts, FTIR Ellipsometry study on RF sputtered Permalloy-oxide Thin Films, MRS Advances 1, 49 (2016), pp. 3361-3366.
[24] Anish Chhaganial Ganhi, R. Pradeep, Yu-Chen Yeh, Tai-Yue Li, Chi-Yuan Want, Y. Hayakawa, Sheng Yun Wu, “Understanding the magnetic memory effect in Fe-Doped NiO Nanoparticles for the Development of Spintronic Devices”, ACS Appl. Nano Mater 2 (2019), 278-290.
[25] P. Mallick, Chandana Rath, R. Biswal, N.C. Mishra, “Structural and Magnetic properties of Fe doped NiO”, Indian J. Phys. 83 (4) 517-523 (2009).
[26] Shankar Acharya, Brian Collier, Wilhelmus J. Geerts, Dual Beam Modulated Magneto-Optical Measurement Setup, accepted for publication in Review of Scientific Instruments (November 2019).
[27] Md. Abdul Ahad Talukder, Wilhelmus J. Geerts, “Tilt angle dependence of the modulated interference effect in Photo-elastic Modulators”, AIP Advances 7, 5 (2017) 056719 1-4; doi: 10.1063/1.4975999.
[28] 7. Md. Abdul Ahad Talukder, Wilhelmus J. Geerts, “Jones matrix description of Fabry-Perot interference in a single axis photoelastic modulator and the consequences for the magneto-optical measurement method.”, AIP Advances 7, 8 (2017) 085320, https://doi.org/10.1063/1.4999517.
[29] Kazuro Kuroda, Takuya Satoh, Sung-Jin Cho, Ryugo Lida, Tutomu Shimura,”Measurement of inverse Faraday effect in NiO using ultrashort laser pulses”, Proc. of SPIE 7728, 77281Z (2010)
[30] A. H. Berg, G. S. Sahasrabudhe, R. A. Kerner, B. P. Rand, J. Schwartz, and J. C. Sturm, “Electron-blocking NiO/crystalline n-Si heterojunction formed by ALD at 175°C,” *Device Res. Conf. - Conf. Dig. DRC*, vol. 2016-Augus, pp. 1–2, 2016.
[31] M.A. Lampert and P. mark, Current Injection in Solids. New York: Academic Press Chapter 2, 1970.

[32] G. Ma, X. Tang, H. Su, H. Zhang, J. Li, and Z. Zhong, “Effects of electrode materials on bipolar and unipolar switching in NiO resistive switching device,” *Microelectron. Eng.*, pp 17-20, volume 124, 2014.
[33] X. Yan, Y. Li, J. Zhao, Y. Xia, M. Zhang, and Z. Liu, “Resistive switching model change induced by electroforming in α-Fe_2O_3 films,” *Phys. Lett. Sect. A Gen. At. Solid State Phys.*, pp, 2392-2395, Vol. 379, Issue 38, 2015.
[34] K. C. Kao, *Dielectric Phenomena in Solids*. Chapter 5, 2004.
[35] Shankar Acharya, “Dual Beam Detection Technique to Study Magneto-Optical Kerr effect”, thesis Texas State University, San Marcos, May 2019.
[36] G. Kresse and J. Furthmuller, “Efficient iterative schemes for ab initio total-energy calculations using a plane-wave basis set”, Phys. Rev. B. 54 (1996) 11169.
[37] P. Blochl, “Projector augmented-wave method”, Phys Rev. B 50 (1994) 17953.
[38] J. Perdew, K. Burke, M. Ernzerhof, “Generalized gradient approximation made simple”, Phys. Rev. Lett. 77 (1996) 3865.
[39] S.L. Dudarev, S.Y. Savrasov, C.J. Mumphreys, and A. P. Sutton, “ Electron-energy-loss spectra and the structural stability of nickel oxide: An LSDA+U study”, Phys. Rev. B 57 (1998) 1505.
[40] John Petersen, Luisa M. Scolfaro, Pablo D. Borges, Wilhelmus J. Geerts, “Symmetry consideration on band filling and first optical transition in NiO”, Eur. Phys. J. B (2019): 92:232, https://doi.org/10.1140/epjb/e2019-100363-5.
[41] Sohee Park, Hyo-Shi Ahn, Choong-Ki Lee, Hanchul Kim, Hosub Jin, Hyo-Sug Lee, Sunae Seo, Jaejun Yu, Seungwu Han, “Interaction and ordering of vacancy defects in NiO”, Phys. Rev. B **77**, 124103-1 124103-7 (2008).
[42] Wei Chen, Yinghui Wu, Jing Fan, Aleksandra B. Djurisic, Fangzhou Liu, Ho Won Tam, Annie Ng, Charles Surya, Wai Kin Chan, Dong Wang, Zhu-Bing He, “Understanding the doping effect on NiO: Toward High-Performance Inverted Perovskite Solar Cells”, Adv. Energy Mater. 8 (2018) 1703519 (1-10).
[43] James Shook, Luisa M. Scolfaro, Pablo D. Borges, Wilhelmus J. Geerts, “Structural stability and electronic properties of XTO2 (X=Cu, Ag; T=Al, Cr): An ab initio study including X vacancies and Mg doping”, Solid State Sciences 88 (2019) pp. 48-56.
[44] James Shook, Pablo D. Borges, Luisa M. Scolfaro, Wilhelmus J. Geerts, “Effects of vacancies and p-doping on the optoelectronic properties of Cu- and Ag-based transparent conducting oxides”, J. Appl. Phys. 126 (2019) 075702.
[45] James Shook, “First Principles Study on the Effects of Vacancies and Mg Doping on the Physical Properties of $CuAlO_2$, $AgAlO_2$, $CuCrO_2$, and $AgCrO_2$, transparent Conductor Oxides”, thesis Texas State University San Marcos, August 2018.
[46] Wilhelmus J. Geerts, Binod D.C., Erik Samwel, Invention disclosure Texas State University, “Automated sample positioning system for a Vibrating Sample Magnetometer employing a modified Mallinson Coil Set”, December 2019.